Robust Multi-objective Optimization of Rare Earth Element Chromatography

Knutson, Hans-Kristian

2016

Document Version:
Other version

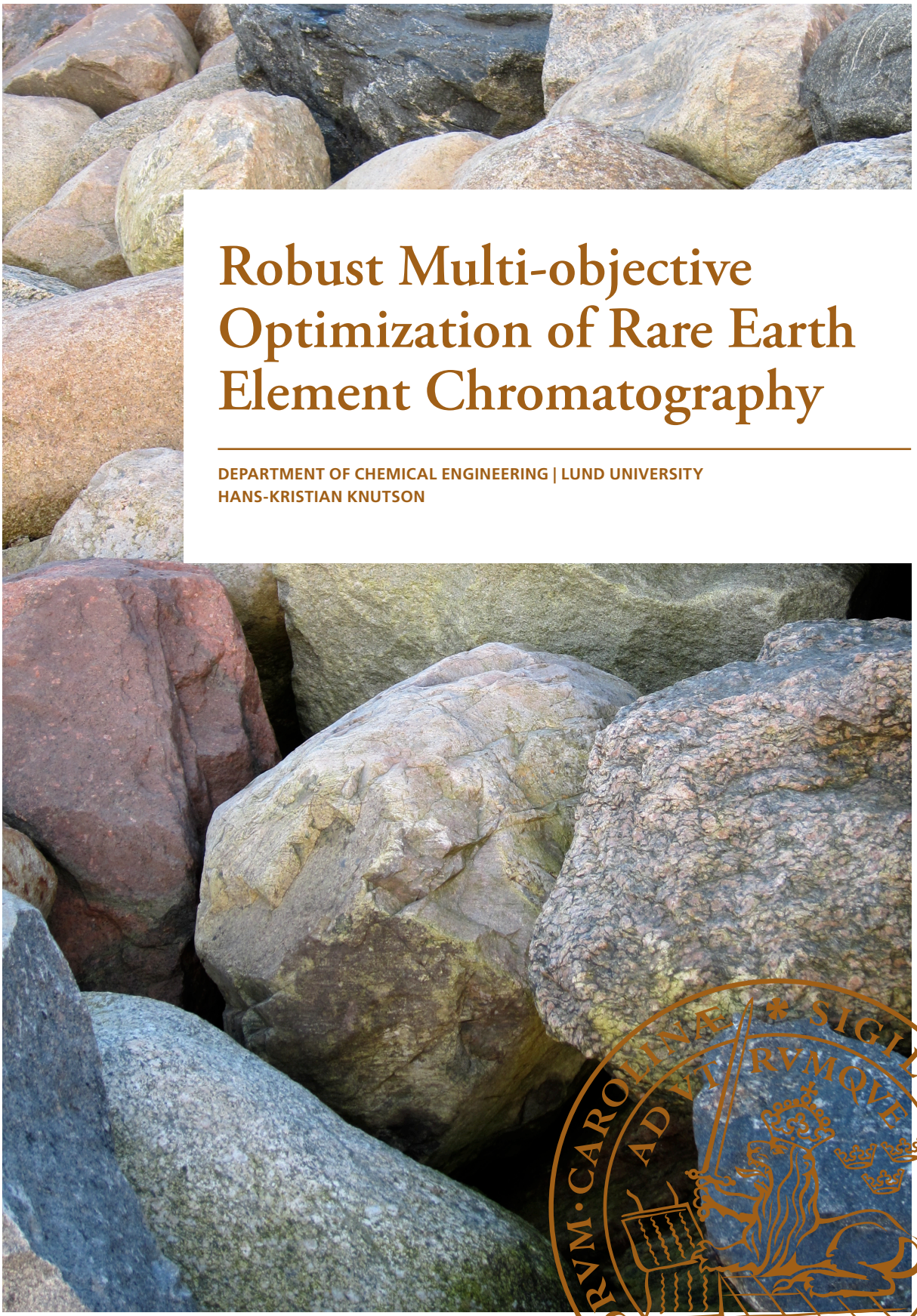

Robust Multi-objective Optimization of Rare Earth Element Chromatography

DEPARTMENT OF CHEMICAL ENGINEERING | LUND UNIVERSITY
HANS-KRISTIAN KNUTSON

Robust Multi-objective Optimization of Rare Earth Element Chromatography

Hans-Kristian Knutson

Department of Chemical Engineering
Lund University, Sweden

2016

ACADEMIC THESIS

which, by due permission of the Faculty of Engineering of Lund University will be publicly defended on 2nd september at 10 am in Lecture hall K:B at the Center for Chemistry and Chemical Engineering, Naturvetarvägen 14, Lund, for the degree of Doctor of Philosophy in Engineering.

The faculty opponent is Professor José Paulo Mota, Universidade Nova de Lisboa, Portugal.

LUND
UNIVERSITY

Organization LUND UNIVERSITY Department of Chemical Engineering P.O. Box 124 SE-221 00 LUND, SWEDEN	**Document name** DOCTORAL DISSERTATION **Date of issue** June 3rd, 2016 **Sponsoring organizations** Swedish foundation for strategic research (SSF), K.A. Rasmussen AS, Process Industry Centre Lund University (PICLU), Production optimization of complex and dynamic processes (ProOpt), Process industrial IT and automation (PiiA), Swedish Governmental Agency for Innovation Systems (VINNOVA)
Author(s) Hans-Kristian Knutson	

Title and subtitle

Robust Multi-objective Optimization of Rare Earth Element Chromatography

Abstract

This thesis contributes to the work of developing chromatography as a rare earth element separation process method. The main focus involves process optimization, *i.e.* studying how the separation process should be operated to achieve the best possible outcome in terms of objectives such as productivity and yield. This has been done through experimental studies on chromatographic rare earth element separation, and to a large extent by applying optimization methods in conjunction with experimentally validated mathematical chromatography models. The findings have provided data regarding expected performance for chromatography as a rare earth element processing method, general operation point strategies when considering conflicting process objectives, as well as the impact of process disturbances and how this can be accounted for by introducing optimization robustness.

Key words

Chromatography, Rare earth elements, Modeling, Multi-objective optimization, Robust optimization

Classification system and/or index terms (if any)

Supplementary bibliography information		**Language** English
ISBN (print) 978-91-7422-447-4		**ISBN (pdf)** 978-91-7422-448-1
Recipient's notes	**Pages** 128	**Price**
	Security classification	

Distribution by (name and address): Department of Chemical Engineering, Lund University
P.O. Box 124, SE-221 00 Lund, Sweden

Signature: Hans-K Knutson **Date:** May 20th, 2016

Robust Multi-objective Optimization of Rare Earth Element Chromatography

Hans-Kristian Knutson

Department of Chemical Engineering
Lund University, Sweden

2016

LUND
UNIVERSITY

Robust Multi-objective Optimization of Rare Earth Element Chromatography

Printed by Media Tryck, Lund University, Lund, 2016

Department of Chemical Engineering
Lund University
P.O. Box 124
SE-221 00 LUND, SWEDEN

ISBN 978-91-7422-447-4 (print)
ISBN 978-91-7422-448-1 (pdf)

“*We don’t make mistakes. We just have happy accidents.*”

Bob Ross

Abstract

Rare earth elements comprise the metallic elements known as lanthanides as well as scandium and yttrium. They are extensively used in modern technological industries and are considered as strategic commodities in many countries. Rare earth element minerals with varying compositions are found at deposits throughout the world, though most of the global REE supply comes from only a few sources. The current industry standard is to employ liquid-liquid extraction methods to separate the elements and upgrade them to suitable purity levels for commercial applications. Chromatography has historically mainly been used as a final purification method, but it is developing to become an alternative separation method with benefits such as achieving higher purity levels, reducing the number of separation steps and utilizing less extractants compared to liquid-liquid extraction. This study is intended as a contribution to the work of developing chromatography as a rare earth element separation method, and focuses on optimization of chromatographic separation on a preparative scale. This has been done through experimental work, and to a large extent by applying optimization methods in conjunction with experimentally validated mathematical chromatography models.

In the experimental optimization work, an overloaded one-step separation of the rare earth elements samarium, europium and gadolinium was accomplished through preparative ion-exchange high-performance liquid chromatography with an bis(2-ethylhexyl) phosphoric acid impregnated column and nitric acid as eluent. The main focus was to optimize the productivity rate, subject to a yield requirement of 80% and a purity requirement of 99% for each element, by varying the flow rate and batch load size. The optimal productivity rate was found to be 1.32 $\mathrm{kg\,samarium/m^3_{column},h^{-1}}$, 0.38 $\mathrm{kg\,europium/m^3_{column},h^{-1}}$ and 0.81 $\mathrm{kg\,gadolinium/m^3_{column},h^{-1}}$.

The model based optimizations have involved the separation of europium from a mixture of the middle rare earth elements samarium, europium and gadolinium as well as the separation of thulium from a heavy rare earth element mixture containing most of the elements. The results from the thulium batch separation showed that a productivity ranging between 0.1-0.45 $\mathrm{kg/m^3_{column},h^{-1}}$ for yields between 73-99% can be expected under a purity constraint of 99%. The findings from the europium batch separation optimization were used to provide with a general strategy for achieving desirable operation points, resulting in a productivity ranging between $0.61 - 0.75$ $\mathrm{kg\ europium/m^3_{column},h^{-1}}$ and a pool concentration between $0.52 - 0.79$ $\mathrm{kg\ europium/m^3}$, while maintaining a purity above 99% and never falling below an 80% yield for the target component.

In addition to this, a comparative study indicated that the performance of the batch separations can be improved by employing continuous multicolumn countercurrent solvent

gradient purification chromatography due to its nature of being a continuous process and its ability to lower the solvent consumption through internal recycling.

Finally, the impact of process disturbances was investigated for the europium batch separation process in conjunction with a robust optimization study. The results from the robust optimization were used to chart the required operation point changes for keeping the amount of failed batches at an acceptable level when a certain level of process disturbance was introduced. It was found that the process is very sensitive towards disturbances and a productivity loss in the range of 10-20% can be expected when accounting for robustness.

Populärvetenskaplig sammanfattning

De sällsynta jordartsmetallerna utgörs av en grupp metalliska grundämnen som kallas lantanoider samt skandium och yttrium. De är viktiga ämnen som används i flera av våra nutida teknologiska produkter. De finns i allt ifrån vardagliga saker som mobiltelefoner, lampor, datorer och bilar till andra lite mer ovanliga användningsområden som lasrar, magneter, katalysatorer och lättviktslegeringar inom flygindustrin. Att dom kallas sällsynta är lite missvisande eftersom de finns i stora mängder på vår planet. Däremot förekommer dom endast i små halter i de mineraler man utvinner metallerna ifrån. Just nu står Kina för den största framställningen, men utvinning förekommer även i Australien, Ryssland och Nordamerika.

Framställningsprocessen är avancerad och det ställs höga renhetskrav på metallerna eftersom deras användningsområden oftast inte tolererar annat än en väldigt ren metallsammansättning. Först krossas mineralerna till en mindre storlek och utsätts sedan för olika kemiska behandlingar tills en vätskelösning som innehåller en blandning av de sällsynta jordartsmetallerna erhålls. Metallerna i denna blandning måste sedan separeras och vanligtvis använder man sig av en metod som kallas vätskeextraktion för att åstadkomma detta. I stort sett utnyttjar vätskeextraktion det fenomen man kan se när man häller olivolja i ett glas vatten och det bildas två skikt, och metallerna kommer att gå från ena skiktet till det andra under extraktionen. Metallseparationen är väldigt utmanande eftersom alla metallerna är väldigt lika både fysiskaliskt och kemiskt, och det gör det svårt att skapa ett tillstånd där en metall inte befinner sig i samma skikt som de andra. Detta är inte lätt att få till exakt och vanligtvis krävs det att man gör flera hundra, och ibland tusentals, extraktionssteg innan man lyckas isolera metallerna var för sig. Vätskeextraktion är en process som lyckas utföra separationen på ett bra sätt, men det finns vissa betänkligheter. Processen använder väldigt många steg och är väldigt energikrävande vilket leder till stora koldioxidutsläpp. Dessutom används stora mängder organiska lösningsmedel som oftast är miljöfarliga och det finns risk för skadliga utsläpp av dessa.

Det finns alternativ till att använda vätskeextraktion som separationsprocess, och det är här denna studien kommer in i sammanhanget. Studien är en del av utvecklingen kring att använda kromatografi som separationsmetod för sällsynta jordartsmetaller. Man kan genom att använda kromatografi uppnå en väldigt bra separation, och oftast även bättre, jämfört med vätskeextraktion. Dessutom kan man minska antalet processteg och behovet av organiska lösningsmedel kan minskas kraftigt. Kromatografiprocessen börjar med att man låter en lösning med metalljoner flöda igenom en så kallad kromatografikolonn, och

då kommer metallerna att fastna och stanna kvar i kolonnen. Sedan låter man en syra flöda genom kolonnen, och genom att öka syrans styrka får man metallerna att släppa efter hand. Ifall man ökar syrans styrka på rätt sätt så kommer bara en viss metallsort att släppas loss och de andra stannar kvar. Detta upprepar man tills man fått alla metallerna att släppa i separerade grupper.

I denna studien visas det bland annat på hur kromatografi kan användas som separationsmetod genom experiment i laboratorieskala. Vidare undersöks det hur kromatografiprocessen kan köras så effektivt som möjligt, både genom experiment och modellbaserade optimeringsstudier. En modellbaserad studie innebär att man har lyckats skapa en matematisk modell med flera ekvationsamband som sedan kan simulera separationsprocessen i den verkliga kromatografi- kolonnen genom datorberäkningar. Detta gör att man inte behöver utföra tusentals experiment för att hitta dom optimala driftspunkterna för processen, utan istället gör tillräckligt med experiment för att säkerställa att den matematiska modellen stämmer bra. Sedan kan man utföra nästan oändligt många experiment genom datorsimuleringar, vilket sparar enormt mycket tid och framförallt resurser.

Själva processoptimeringen har i detta sammanhanget inneburit att ta reda på hur driftsparametrarna, som till exempel syrans styrka, ska ställas in för att få ett så bra processresultat som möjligt. Vad som är ett bra processresultat är tyvärr inte alltid entydigt, och man ställs ofta inför en situation där man både vill äta kakan och behålla den. De flesta känner säkert igen situationer då man måste bestämma ifall man vill göra något snabbt, ifall det ska göras mycket noggrant, eller ifall det finns någon bra kompromiss mellan tidsåtgång och noggrannhet. Just denna problemställningen blir väldigt reell när man optimerar en kromatografiprocess. Antingen kan man få en väldigt hög produktionshastighet av separerade metaller, men då kommer tyvärr utbytet att minska avsevärt och man får ett stort spill. Eller så kan man se till att man får ett väldigt litet spill, men då kommer processen att ta väldigt lång tid och ge en alltför låg produktionshastighet. Både spill och produktionshastighet kan ses som ekonomiska termer som har en inbördes påverkan, och det gäller att hitta en balans mellan dessa i förhållande till hur man värderar tid och spill. I denna studien kartläggs den inbördes påverkan mellan olika processresultat för att underlätta beslutsfattandet kring en lämplig balanspunkt, och dessutom kartläggs det hur driftsparametrarna ska ställas in för att uppnå det man anser vara optimalt processresultat. Slutligen har det även undersökts hur processen påverkas vid processtörningar, och hur man redan vid processoptimeringen kan ta hänsyn till förväntade processtörningar för att hitta driftsparametrar som kan hantera en viss störningsnivå med bibehållen produktkvalitet.

Acknowlegements

Firstly, the financial support from the Swedish foundation for strategic research (SSF), Process Industry Centre Lund University (PICLU), Production optimization of complex and dynamic processes (ProOpt), Process industrial IT and automation (PiiA), K.A. Rasmussen AS and the Swedish Governmental Agency for Innovation Systems (VINNOVA) is gratefully acknowledged.

There are many persons that have given me support throughout my time as a PhD student, both professionally and by being awesome people that make the state of things feel plainly sweet. I sincerely hope that you all feel I return the appreciation and love you deserve, and I would like to drop a few names and shoutouts here.

I would like to start by thanking my supervisor Bernt Nilsson for all the support, insightful discussions and good times. Without you, this thesis would not have come to be. I also want to thank my co-supervisor Anders Holmqvist for your support when math got heavy and your availability for fruitful discussions on both factual and intangible matters.

I owe many thanks to my colleagues at the Department of Chemical Engineering and to especially name a few; Anton for all the über-awesome discussions and your understanding of science, Mark for all the good times on and off a board, Niklas Borg for support at the beginning of my studies and the evening gaming sessions, Niklas Andersson for help with the cluster and other scientific matters, Fredrik Nielsen for all the talks, Josefine Hagman for the great times when we shared office, Christian Jönsson for our excellent time in the lab, Maria for all the help with administrative matters, and finally I would like to express my gratitude to Karolina, Jonas, Mikael and Hamse for the good times.

There are many friends that I owe big thanks to, and I would like to start with a big spasiba to the entire Roskilde black carrot camp family including notoriously good people like Estelle, Anders, Hille, Thuring, Ida, Krille H, Thomas, Evy, Poy, Robin, Moa and Metal just to name some of the major players. I would also like to extend a huge thanks and love to the team of super good friends *a.k.a.* surfpågarna or stugangänget; Ola, Danne, Rick, Joël, Martin, Magic Perfectson and Elias.

I want to thank and convey love to my family, especially Anita, Dolf and Karl-Axel for all the support, understanding and just being there for me. I also want to thank my extended family from the deep woods of Värmland for making the world feel like a warmer place.

Finally and foremost, I want to thank Frida for all the love and support. You keep me stoked and you make my heart tick harder <3

May 2016, Lund
Hans-Kristian Knutson

Contents

Preface . . . . . **ix**
Contents and contributions of the thesis ix
1. Introduction **1**
1.1 Rare earth elements 1
1.2 Rare earth element processing 1
1.3 Aim and scope 2
2. Chromatographic separation of rare earth elements **3**
2.1 Chromatography 3
2.2 Chromatographic separation techniques 4
2.3 Experimental chromatography system description 7
3. Mathematical modeling of chromatography **9**
3.1 Column model 9
3.2 Simulation methods 12
3.3 Parameter estimation 13
3.4 Modeling results 14
4. Multi-objective optimization **17**
4.1 Optimization 17
4.2 Multi-objective optimization problem 20
4.3 Optimization methods 21
4.4 Optimization results 22
5. Robust multi-objective optimization **27**
5.1 Robust optimization 27
5.2 Robust counterpart problem formulation 28
5.3 Robust optimization method 29
5.4 Results from robust multi-objective optimization 29
6. Conclusion **35**
6.1 Summarizing conclusions 35
6.2 Future work 35
Bibliography **37**
Paper I. Experimental productivity rate optimization of rare earth element separation through preparative solid phase extraction **45**
Paper II. Multi-objective optimization of chromatographic rare earth element separation **53**

Paper III. Model-based comparison of batch and continous preparative chromatography in the separation of rare earth elements **63**

Paper IV. Modeling preparative chromatographic separation of heavy rare earth elements and optimization of thulium purification **79**

Paper V. Robust multi-objective optimization of chromatographic rare earth element separation **93**

Preface

Contents and contributions of the thesis

This thesis consists of six chapters and five papers. This section comprises a brief description of the six chapters, each paper and the contributions made by the author. The papers are appended at the end of the thesis.

Chapter 1—Introduction

This chapter provides a brief overview of rare earth elements and rare earth element processing as well as the aim and scope of this thesis.

Chapter 2—Chromatographic separation of rare earth elements

This chapter highlights chromatographic separation techniques in the context of rare earth element separation and provides information regarding the chromatography system configuration used in this work.

Chapter 3—Mathematical modeling of chromatography

This chapter concerns methods for accomplishing simulations of chromatographic rare earth separation.

Chapter 4—Multi-objective optimization

This chapter provides a method for optimizing chromatographic separation processes with several competing objectives.

Chapter 5—Robust multi-objective optimization

This chapter presents a method for robust optimization of chromatographic separation processes with several competing objectives.

Chapter 6—Concluding Remarks

This chapter concludes the thesis with a brief summary of the results and some suggestions for future work.

Paper I
Knutson, H.-K., Max-Hansen, M., Jönsson, C., Borg, N., and Nilsson, B. (2014). Experimental productivity rate optimization of rare earth element separation through preparative solid phase extraction chromatography. *Journal of Chromatography A*, 1348:47–51

This paper presents an experimental optimization study of batch chromatographic separation of middle rare earth elements. The study provides a chromatography system configuration for achieving the separation as well as performance data.
I planned and performed most of the work, analyzed the results and wrote most of the article.

Paper II
Knutson, H.-K., Holmqvist, A., and Nilsson, B. (2015). Multi-objective optimization of chromatographic rare earth element separation. *Journal of Chromatography A*, 1416:57–63

This paper concerns a multi-objective optimization study for batch chromatographic separation of middle rare earth elements with europium as target product. The study presents a method for parameter estimation and optimization, and provides with expected optimal performance data as well as a general operation point strategy for the separation.
I planned and performed most of the work, analyzed the results and wrote most of the article.

Paper III
Andersson, N., Knutson, H.-K., Max-Hansen, M., Borg, N., and Nilsson, B. (2014). Model-based comparison of batch and continuous preparative chromatography in the separation of rare earth elements. *Industrial & Engineering Chemistry Research*, 53(42):16485–16493

This paper presents a comparative study for multi-objective optimization of batch- and continuous- chromatographic rare earth element separation. The study shows that continuous two-column countercurrent solvent gradient purification is a good alternative to batch chromatography.
I planned and performed most of the experimental work, and helped with analyzing results and writing the article.

Paper IV
Max-Hansen, M., Knutson, H.-K., Jönsson, C., Degerman, M., and Nilsson, B. (2015). Modeling preparative chromatographic separation of heavy rare earth elements and optimization of thulium purification. *Advances in Materials Physics and Chemistry*, 5(05):151

This paper concerns a multi-objective optimization study for batch chromatographic separation of heavy rare earth elements with thulium as target product. The study presents a method for calibration and optimization, and provides with expected performance data for thulium separation.
I assisted with experimental planning, analyzing results and writing the article.

Paper V

Knutson, H.-K., Holmqvist, A., and Nilsson, B. Robust multi-objective optimization of chromatographic rare earth element separation. (Submitted for publication)

This paper presents a robust multi-objective optimization study for batch chromatographic separation of middle rare earth elements with europium as target product. The study presents a method for robust optimization, and provides with a charting of required operation point changes for keeping the amount of failed batches at an acceptable level when a certain process disturbance is introduced.
I planned and performed most of the work, analyzed the results and wrote most of the article.

1

Introduction

1.1 Rare earth elements

The rare earth elements (REE) comprise the lanthanides, *i.e* the elements with atomic numbers 57 through 71 in the periodic system, as well as scandium and yttrium. They are all metallic elements with very similar physical and chemical properties, and they are found in varying types of mineral ores at sites around the world [27, 46]. The denomination '*rare*' is somewhat misleading as they are quite abundant in the earth's crust, and '*rare*' rather relates to that the quantity of REEs in an ore tends to be very low.

REEs are used in many modern technological applications (such as magnets, batteries, catalysts, lamps, monitors, lasers, superconductors, capacitors and aero space alloys), and are considered as strategic commodities in many countries [21, 43, 49, 62]. Before the elements can be used for commercial purposes, they must be upgraded to very high purity levels. This is traditionally achieved through liquid-liquid extraction (LLE) methods [13, 25, 64], but chromatography is on the rise as an alternative method as of lately [26, 35, 38, 40, 45, 51]. There are several benefits with chromatography as a purification method. Chromatography is able to reach higher purity levels than LLE, the extractant expenditure can be lowered, process media can be recycled to a higher extent and the number of separation steps can be substantially reduced [25].

1.2 Rare earth element processing

There are several ways to process REE ore and the process selection will depend on the ore type [25]. As a typical example, a brief scheme for processing Monazite ore is presented in Figure 1.1. This process mainly consists of six steps that produce separated REEs as well as phosphates for fertilizer production as a by-product. First the Monazite ore is ground to a finer size, after which it is mixed with hot caustic soda to dissolve phosphates from the mineral. The phosphates are filtered out and the remaining solution with REE hydroxides is mixed with nitric acid and barium salt. Then there is a second filtering step to remove insoluble radioactive elements and other inert materials. The rare earth nitrates can then be separated into rare earth products by means of LLE, chromatography, or a combination of both.

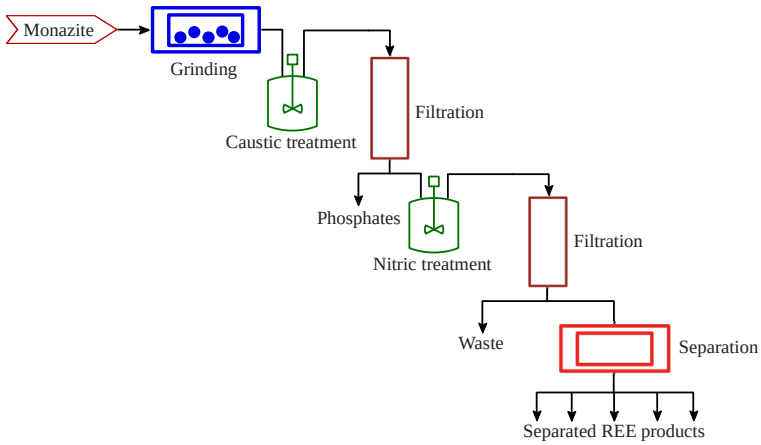

Figure 1.1 Processing of Monazite ore. The process consits of six steps; (1) grinding, (2) caustic treatment, (3) filtration, (4) nitric treatment, (5) filtration, and (6) separation of REEs.

1.3 Aim and scope

The aim of this thesis is to contribute to the work of developing chromatography as a rare earth element separation process method. The main focus involves process optimization, *i.e.* studying how the separation process should be operated to achieve the best possible outcome in terms of objectives such as productivity and yield. This has been done through experimental studies on REE separation, and to a large extent by applying optimization methods in conjunction with experimentally validated mathematical chromatography models. The findings have provided data regarding expected performance for chromatography as a REE processing method, general operation point strategies when considering conflicting process objectives, as well as the impact of process disturbances and how this can be accounted for by introducing optimization robustness.

2

Chromatographic separation of rare earth elements

2.1 Chromatography

Chromatography is a separation technique that is used for analytical and preparative purposes. In analytical chromatography, the objective is to analyze the composition of a mixture and the sample size is small, whereas preparative chromatography is used for purification of components in larger capacity. The separation is achieved by letting a mixture flow through a column that is packed with particles referred to as the stationary phase. The particles are porous and have a backbone which is coated with ligands that interact with the desired target components in the mixture. When the mixture is loaded into the column, the conditions in the column are set to allow for a high interaction between the components and the ligands so that the components bind to the ligands. After the column has been loaded, the conditions are changed so that some components start eluting while some components are still retained. The conditions can be changed through several steps or by a gradient to achieve the desired level of separation between the components. The flow with eluted components can be collected in product pools or sent to a waste container by means of a valve. A chromatogram, which is the column outlet component concentration profile, is used for deciding the cut-points that dictate when the valve directs the outlet stream to a product pool or to the waste. The transport phenomena involved in the separation can be divided into two levels as depicted in Figure 2.1; (*i*) the bulk transport which is mainly due to convection, and (*ii*) the stationary phase mass transfer that concerns component interaction with the ligands and intra-particle diffusion.

2.1.1 Rare earth element chromatography

In the context of REE chromatography, the separation can be achieved through extraction chromatography where the ion-exchange interaction between the elements in the mobile phase and the immobilized ligands is exploited by means of acid modifiers. Alternatively, there is also the option to use a ligand-assisted elution chromatography scheme [40] where ligands are present in the mobile phase and compete with the ligands on the stationary phase to form a mobile phase ligand-REE complex.

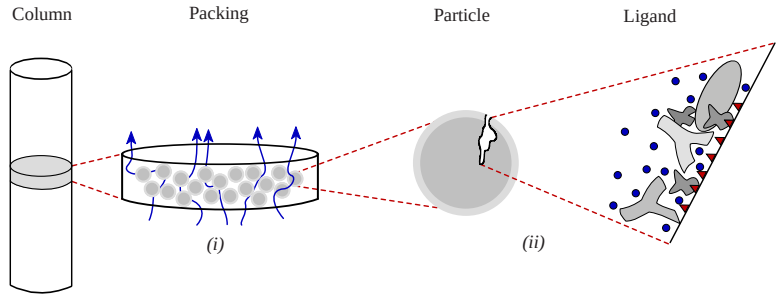

Figure 2.1 The transport phenomena involved in the separation can be divided into two levels; (*i*) the bulk transport, and (*ii*) the stationary phase mass transfer.

Various ligands, such as bis(2-ethylhexyl) phosphoric acid (HDEHP), ethylenediaminetetraacetic acid (EDTA), 2-ethylhexyl phosphonic acid (HEHEHP) and di-(2,4,4-trimethylpentyl) phosphinic acid (DT- MPPA) can be used for extraction chromatography. The modifier is typically an acid, such as nitric acid, hydrochloric acid or α-Hydroxyisobuturic acid (α-HIBA), that affects the REE-ligand interaction according to an equilibrium generally described as:

$$\mathrm{REE}^{3+} + \mathrm{H_3} \cdot \mathrm{Ligand} \rightleftharpoons \mathrm{REE} \cdot \mathrm{Ligand} + 3\mathrm{H}^{+}.$$

In this work, nitric acid was used as a modifier and HDEHP was preferred as ligand due to its proven suitability from both liquid-liquid extraction processes [25, 64] as well as chromatography [8, 28, 31, 35, 51, 55, 57, 59]. HDEHP also offers a very good resolution for light to medium REEs (*i.e.* lanthanum to gadolinium) [52] which comprise the majority of REE separations studied in this work.

2.2 Chromatographic separation techniques

Chromatography can be carried out batch-wise or continuously. There are several continuous chromatography methods such as multicolumn countercurrent solvent gradient purification (MCSGP), simulated moving bed (SMB) and developments of the SMB process principle including VariCol, PowerFeed, iSMB, and R-SMB to mention a few [53, 56]. SMB utilizes a series of columns with periodically moving inlet and outlet ports to achieve a simulated counter current movement of the mobile- and stationary- phase [14, 47]. MCSGP combines batch and SMB chromatography by using several columns that are switched in position opposite to the flow direction [3]. Some columns are interconnected to allow for internal countercurrent recycling of impure product streams, some columns are operated in batch mode, and the modifier concentration at the column inlets can be adjusted by utilizing individual gradient pumps.

The techniques involved in this work are batch chromatography, as in Paper I-V, and two-column MCSGP as in Paper III.

2.2.1 Batch chromatography

The general schematics for batch chromatography is presented in Figure 2.2, and the process is illustrated in Figure 2.3. It mainly consists of three steps; First the column is loaded with a feed mixture. After the loading step, a modifier is used to elute the components either through isocratic-, gradient- or step- elution. During the elution step, the flow from the column outlet is either diverted to product collection or sent to the waste by means of a valve. Finally, the column is regenerated and re-equilibrated after which the column is ready for another batch load.

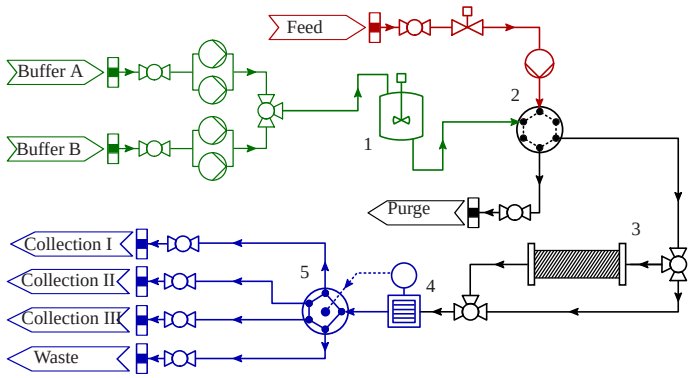

Figure 2.2 General schematics for a batch chromatography process. (1) Buffer mixing, (2) switching valve, (3) column, (4) detector, and (5) fractionizing valve.

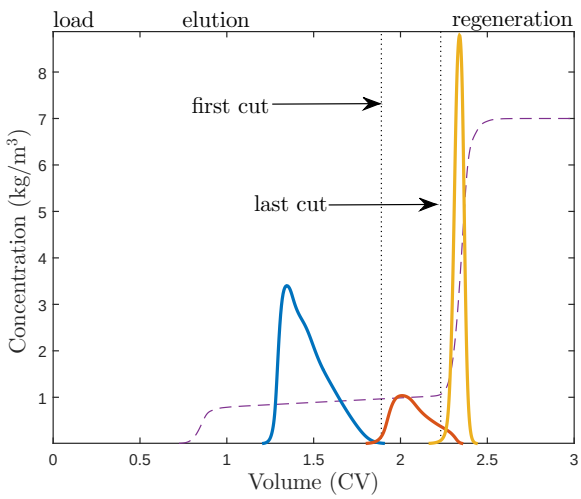

Figure 2.3 Batch chromatography with a load-, elution- and regeneration- step. The colored peaks indicate the concentration profile of each component at the column outlet. The dashed line indicates the modifier concentration. The dotted lines indicate the cut times when the flow is diverted to the product collection. The regeneration step is followed by a wash step to re-equilibrate the column.

2.2.2 Two-column MCSGP

Two-column MCSGP can arguably be regarded as a semi-continuous process. The general schematics for a two-column MCSGP configuration is presented in Figure 2.4, and the process is illustrated in Figure 2.5.

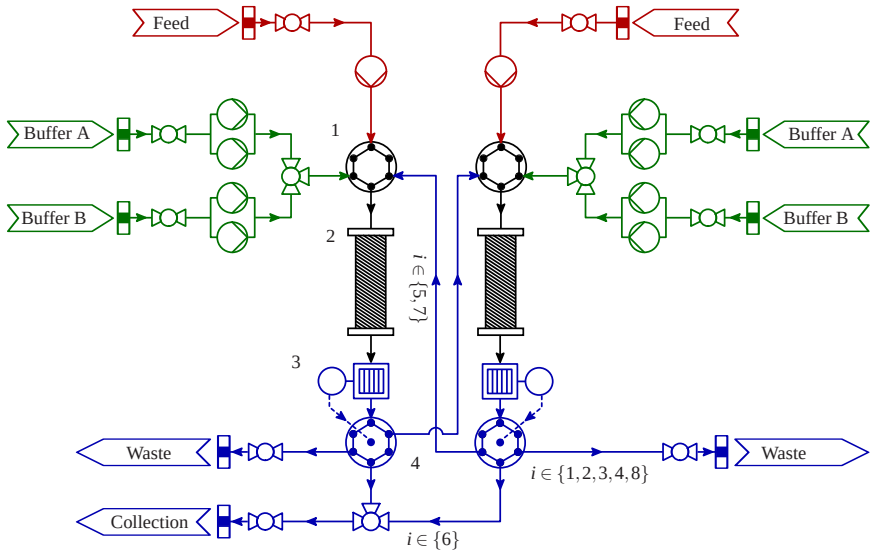

Figure 2.4 General schematics for a two-column MCSGP configuration. (1) switching valve, (2) column, (3) detector and (4) fractionizing valve. The index $i \in [1..8]$ denotes the individual temporal sections of a full cycle.

The process is run in two interconnected steps, I_1 and I_2, and two batch steps, B_1 and B_2, as indicated in Figure 2.5. The process cycle can be divided into eight different temporal sections, s_{1-8}, that together form a complete chromatogram. Here, the process is explained in the context of Paper III which involves the separation of europium (Eu), as target product (P), from samarium (Sm) and gadolinium (Gd) that respectively are considered as weakly- (W), and strongly- (S), adsorbed impurities.

During the first interconnected step, column 1 is running in section s_1 simultaneously with column 2 in section s_5. Column 1 is loaded with W and P from the column 2 outlet, and the column 1 outlet is sent to the waste. During the first batch step (s_2 and s_6 are run simultaneously) column 1 is loaded with fresh feed and the target product is eluted from column 2 and sent to collection. During the second interconnected step (sections s_3 and s_7 are run simultaneously), column 1 is loaded with P and S from the column 2 outlet and the column 1 outlet is sent to waste. Finally, both columns are eluted during the second batch step which includes the temporal sections s_4 and s_8. At this point, the column 1 outlet contains most of W, the column 2 outlet consists of S, and both column outlets are sent to the waste. After the second batch step, the two columns are switched so that column 1 begins the following cycle in section s_5, and column 2 in s_1.

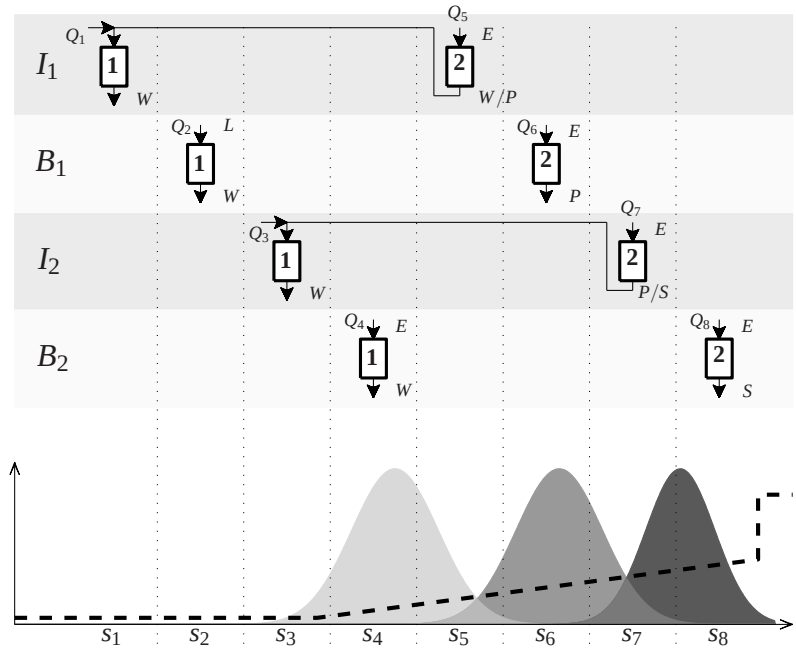

Figure 2.5 Process description of two-column MCSGP. The process is run in two interconnected steps, I_1 and I_2, and two batch steps, B_1 and B_2. The eight temporal sections, s_{1-8}, form a complete chromatogram. The flows for each corresponding section are denoted Q_{1-8}. The fresh load (L) is introduced in s_2, the weakly adsorbed impurities (W) are sent to waste in s_1-s_4, the product (P) is collected in s_6, and the strongly adsorbed impurities (S) are sent to waste in s_8. The elution (E) steps are indicated in the figure, and the elution order is W, P, and S.

2.3 Experimental chromatography system description

An Agilent 1260 Bio-Inert HPLC system with two Agilent 1260 Bio-Inert quaternary pumps and an Agilent Bio-Inert 1260 auto-sampler was used for the experimental batch chromatography work in Paper I-IV. The in-line post column REE detection was performed with an Agilent 7700 inductively coupled plasma mass spectrometry (ICP-MS) system since ICP-MS has a good capability for REE dectection [11, 13, 28]. Kromasil columns were delivered as is with a stationary phase consisting of spherical silica particles coated with C18, a diameter of 16 μm and a pore size of 100 Å. A GE Healthcare ÄKTA Purifier 100 was used for preparing the columns with HDEHP ligands.

3

Mathematical modeling of chromatography

3.1 Column model

Computer modeling is an efficient tool for evaluating the performance of a system, and the lowered resource expenditure through reduced need for experimental work is a notable benefit. The method involves a mathematical model that, together with model parameters that have been estimated in accordance to experimental observations, is capable of describing the dynamics of the studied system. Once the model parameters have been estimated, the model can be employed to predict the system behaviour which in the case of chromatographic separation means the column dynamics.

The column model describes the transport of the injected particles through the chromatography column, and is utilized to obtain the time varying concentration profiles. There are two transport phenomena that need to be considered; (*i*) the bulk transport which is mainly due to convection, and (*ii*) the stationary phase mass transfer as depicted in Figure 2.1. The most elementary way to describe the bulk transport is to employ the ideal model [24]. However, the ideal model does not consider dispersion and for this reason the convective-dispersive model [24] is preferred in this work. The stationary phase mass transfer concerns intra-particle diffusion and component interaction with the ligands. The intra-particle diffusion is assumed to not be rate limiting and only have a minimal impact on the transport dynamics, given the size of the components and the particles. The rare earth element adsorption to the ligands, that are immobilized on the column particles, is represented by adding a kinetic term to the convective-dispersive model. The lanthanides are assumed to have an ion-exchange interaction with the ligands [35, 39], and these kinetics can be described by a steric mass-action (SMA) model [12], or a Langmuir mobile phase modulator (MPM) model [22, 23, 34].

In this work (Paper II-V), a kinetic convective-dispersive model [24, 53] with a Langmuir MPM isotherm [32, 34, 45, 51] was used to describe the column separation as it provides with good model accuracy at a reasonable computational cost. The model equations, defined in the spatial, $z \in [z_0, z_f]$, and temporal, $t \in [t_0, t_f]$, domains are formulated as:

$$\frac{\partial c_\alpha}{\partial t} = -\frac{\partial}{\partial z}\left(c_\alpha v_{\text{int}} - \mathscr{D}_{\text{app},\alpha}\frac{\partial c_\alpha}{\partial z}\right) - \frac{(1-\varepsilon_c)}{\varepsilon_c + (1-\varepsilon_c)\varepsilon_p}\frac{\partial q_\alpha}{\partial t}, \tag{3.1}$$

$$\frac{\partial q_\alpha}{\partial t} = k_{\text{kin},\alpha}\left(c_\alpha K_{eq,\alpha} q_{max,\alpha}\left[1 - \sum_{\gamma\in\{\text{REE}\}}\frac{q_\gamma}{q_{\text{max},\gamma}}\right] - q_\alpha c_S^{\nu_\alpha}\right), \tag{3.2}$$

where c_α and q_α are the mobile and solid phase concentration of component α, v_{int} is the quotient of superficial velocity over total porosity, $\mathscr{D}_{\text{app},\alpha}$ the apparent dispersion coefficient, and ε_c and ε_p the column and particle void fractions. Here, c_S denotes the concentration of the modifier and $k_{\text{kin},\alpha}$ is a lumped parameter describing the film transport, intraparticle diffusion and binding kinetics. $K_{eq,\alpha}$ denotes the equilibirum constant regarding adsorption and desorption, ν_α a parameter describing the ion-exchange characteristics, and $q_{\text{max},\alpha}$ the maximum concentration of adsorbed components. The column model does not consider modifier ions on the solid phase, therefore Eq. (3.2) and its associated part in Eq. (3.1) are omitted (i.e. $\partial q_\alpha/\partial t \equiv 0$) when $\alpha = \text{S}$.

3.1.1 Batch mode formulation

When the column is run in batch mode, Eq. (3.1) is complemented with Danckwert boundary conditions [24]:

$$c_\alpha(t,z_0)v_{\text{int}} - \mathscr{D}_{\text{app},\alpha}\frac{\partial c_\alpha}{\partial z}(t,z_0) = \begin{cases} c_{\text{load},\alpha}v_{\text{int}}\Pi(t,t_0,\Delta t_{\text{load}}) & \text{if } \alpha \in \{\text{REE}\}, \\ c_{\text{mix},S}v_{\text{int}} & \text{if } \alpha = S, \end{cases} \tag{3.3}$$

$$\frac{\partial c_\alpha}{\partial z}(t,z_f) = 0, \qquad \forall \alpha \in \{\text{REE, S}\} \tag{3.4}$$

where $c_{\text{load},\alpha}$ is the injected load concentration, and $\Pi(t,t_0,\Delta t_{\text{load}}) \in \{0,1\}$ a rectangular function in the temporal horizon $[t_0, \Delta t_{\text{load}}]$.

The dynamics of the modifier concentration in the upstream mixing tank, $c_{\text{mix},S}$, are given by:

$$\frac{\mathrm{d}c_{\text{mix},S}}{\mathrm{d}t} = \frac{1}{\tau_{\text{mix}}}\left(u(t) - c_{\text{mix},S}\right), \tag{3.5}$$

$$u(t) = \begin{cases} u_0, & \text{if } t \le \Delta t_{\text{load}} + \Delta t_{\text{wash}}, \\ u_0 + \Delta u(t - (\Delta t_{\text{load}} + \Delta t_{\text{wash}})), & \text{if } t > \Delta t_{\text{load}} + \Delta t_{\text{wash}}, \end{cases} \tag{3.6}$$

where τ_{mix} is the residence time, u is the elution gradient described by the initial value, u_0, and the slope of the linear elution gradient, Δu, expressed as $\Delta u = \frac{u_f - u_0}{t_f - (\Delta t_{\text{load}} + \Delta t_{\text{wash}})}$.

3.1.2 Two-column MCSGP cyclic steady state criteria formulation

The solution for a complete MCSGP time horizon, $t \in [t_0, t_f]$, requires that the model describing the system dynamics is augmented with additional cyclic steady state (CSS) criteria to ensure that the state at the initial time is retained at the end of the cycle. The CSS

can then be established by starting from a set of initial conditions, and simulate the process until CSS is attained according to the desired tolerance level.

For the two-column MCSGP configuration described in Chapter 2, the mixing of the recirculated flows in the temporal sections s_1 and s_3 are described as:

$$0 = r_\alpha(t-0.5t_f) - c_{\alpha,\text{mix}} \sum_{i\in\{1,3\}} \Pi_i(t)\left[\dot{Q}_i + \dot{Q}_{i+4}\right], \tag{3.7}$$

$$0 = r_S(t-0.5t_f) + \sum_{i=1}^{8} \Pi_i(t)\dot{Q}_i\left[(1-u(t))\,c_{\text{Buffer},A} + u(t)c_{\text{Buffer},B}\right] - c_{S,\text{mix}}\left[\sum_{i\in\{1,3\}} \Pi_i(t)\left[\dot{Q}_i + \dot{Q}_{i+4}\right] + \sum_{\substack{i=1\\ i\notin\{1,3\}}}^{8} \Pi_i(t)\dot{Q}_i\right] \tag{3.8}$$

where r_α denotes the mass flow of component α in the stream entering column 1, $c_{\alpha,\text{mix}}$ indicates the concentration when the recirculated stream and Q_i are mixed and Π corresponds to a rectangular function for the given temporal section.

The CSS criteria can be expressed by periodicity constraints. Here, r_α and $\forall\alpha \in \{REE, S\}$, are governed by the equality constraints:

$$0 := r_\alpha(t-0.5t_f) - \sum_{i\in\{5,7\}} \Pi_i(t)\dot{Q}_i c_\alpha(t,z_f), \quad \forall t \in [0.5t_f, t_f]. \tag{3.9}$$

It should be noted that the equality constraints are shifted a half cycle in time. Moreover, in order to ensure that all components $\alpha \in \{REE\}$ are completely eluted at t_f, a terminal equality constraint is added:

$$0 := \left[c_{\text{load},\alpha}\Delta t_{\text{load}}\dot{Q}_2 + \int_{t_0}^{t_f} r_\alpha(t-0.5t_f)\mathrm{d}t\right] - \int_{t_0}^{t_f}\sum_{i=1}^{8}\Pi_i(t)\dot{Q}_i c_\alpha(t,z_f)\mathrm{d}t, \tag{3.10}$$

The equality constraints:

$$0 := c_S(t_0,z) - c_S(t_f,z), \quad z \in [z_0, z_f], \tag{3.11}$$

$$0 := c_{S,\text{mix}}(t_0) - c_{S,\text{mix}}(t_f), \tag{3.12}$$

govern that the modifier concentration, $c_S(t,z)$, at every column position $z \in [z_0, z_f]$ as well as the concentration in the mixing unit, $c_{S,\text{mix}}(t)$, are consistent at the initial and terminal times. Although the periodicity constraints only consider the dynamics of the mobile phase, the dynamics of the stationary phase is inherently comprehended in this formalism.

Finally, the boundary conditions in Eq. (3.3) are replaced with the formulations of Eq. (3.7 and 3.8) for a two-column MCSGP, and given by:

$$c_\alpha(t,z_0)\frac{\dot{Q}(t)}{A_c\varepsilon_{tot}} - \mathscr{D}_{\text{app}}(t)\frac{\partial c_\alpha}{\partial z}(t,z_0) = \begin{cases} c_{\text{load},\alpha}\Pi_{\text{load}}(t)\dfrac{\dot{Q}_2}{A_c\varepsilon_{tot}} + c_{\alpha,\text{mix}}\displaystyle\sum_{i\in\{1,3\}}\frac{\Pi_i(t)}{A_c\varepsilon_{tot}}\left[\dot{Q}_i + \dot{Q}_{i+4}\right] & \text{if } \alpha \in \{REE\}, \\ c_{S,\text{mix}}\dfrac{\dot{Q}(t)}{A_c\varepsilon_{tot}} & \text{if } \alpha = S, \end{cases} \tag{3.13}$$

The time dependencies of the volumetric flow rate, $\dot{Q}$, and the apparent dispersion coefficient, $\mathscr{D}_{\text{app}}$, for a column in a given temporal section are given by:

$$\dot{Q}(t) = \sum_{i\in\{1,3\}} \Pi_i(t)\left[\dot{Q}_i + \dot{Q}_{i+4}\right] + \sum_{\substack{i=1 \\ i\notin\{1,3\}}}^{8} \Pi_i(t)\dot{Q}_i, \tag{3.14}$$

$$\mathscr{D}_{\text{app}}(t) = \frac{\dot{Q}(t)D_p}{A_c\varepsilon_{tot}\text{Pe}}, \tag{3.15}$$

where D_p denotes the particle diameter, A_c the column cross sectional area, and Pe the Peclet number.

3.2 Simulation methods

The column model was implemented in a MATLAB environment via the preparative chromatography simulator (pcs) [9]. The partial differential equations (PDE) were solved by first transforming them into a system of ordinary differential equations (ODE) through spatial discretization. The ODE system could then be solved by utlizing MATLAB's differential algebraic equation (DAE) solver ode15s, which is suitable due to the stiff dynamics of the system. The first-order spatial derivative in Eq. (3.1) was approximated using a method-of-lines and finite volume method with 100 grid points where $z_k = k\Delta z$ is the discretized spatial coordinate and $k \in [1..100]$. The first order derivative was approximated as a two-point backward difference, and the second-order derivative was approximated as a three-point central difference.

3.2.1 Parallel computing

For demanding optimizations, such as in Paper II-V, it becomes necessary to evaluate a massive amount of model simulations. Such computation heavy tasks can be carried out more rapidly by using a parallel computing methodology. A parallel computing methodology as described in [1, 2] was utilized in this work, and a computer cluster consisting of 60 working drone cores, a server and a client, was used to provide an environment for handling parallel simulations. Essentially, the client (*i.e.* the user computer) requests the cluster to perform a computation task, and the server hosts a script that distributes the computation jobs to available drones and organizes the file communication.

3.3 Parameter estimation

Before the column model can be utilized for predictions of the system behaviour, model parameters that provides a good fit between simulation and experimental data must be determined. This is a challenging task that can be carried out by means of the inverse method [10, 16, 20, 33, 54], which involves minimization of the least squares error between the normalized simulated chromatograms and the normalized detector responses from corresponding experiments. Both isocratic- (Paper IV) and linear- (Paper II, III and V) elution gradient experiments were used for the purpose of parameter estimation.

3.3.1 Parameter estimation method

In the work presented in this thesis, the model parameters were estimated through nonlinear parameter estimation by means of the Levenberg-Marquardt algorithm through MATLAB's *lsqcurvefit* wrapper with forward finite differences to estimate the Jacobian. The algorithm minimizes the weighted sum of the deviations between the observed, $\hat{c}$, and predicted, c, system responses, expressed as:

$$\text{min.} \quad \sum_{j=1}^{N_j} [\hat{c}(\hat{t}_j, z_f) - c(\hat{t}_j, z_f, \boldsymbol{p}_j, \beta)]^T \boldsymbol{W}_j [\hat{c}(\hat{t}_j, z_f) - c(\hat{t}_j, z_f, \boldsymbol{p}_j, \beta)], \tag{3.16a}$$

$$\text{w.r.t.} \quad \beta \in \mathbb{R}^{\boldsymbol{N}_\beta},$$

$$\text{s.t.} \quad \dot{\boldsymbol{x}} = \boldsymbol{F}(t, \boldsymbol{x}(t), \boldsymbol{p}, \beta), \quad \boldsymbol{x}(t_0) = \boldsymbol{x}_0, \tag{3.16b}$$

$$\beta_L \leq \beta \leq \beta_U, \tag{3.16c}$$

where j indicates the experiment index, β is a vector containing the parameters being estimated, $\boldsymbol{x}$ denotes the time varying process variables, $\boldsymbol{p}$ gives the process parameters such as load and elution gradient settings, $\boldsymbol{F}$ is the ODE system governed by Eqs. (3.1,3.2,3.5), and $\boldsymbol{W}$ is a diagonal weight matrix introduced to normalize the experimental response and penalize a deviation with its associated variance.

3.4 Modeling results

When the model parameters were estimated, it was possible to predict the chromatography system performance for various process operation points. This was done in the context of linear elution gradient batch chromatography (Paper II, IV and V) and MCSGP (Paper III). The estimated parameters for batch separation of Sm, Eu and Gd (Paper II and V), are given in Table 3.1, and a model response chromatogram is plotted along with the associated experimental data in Fig. 3.1. The MCSGP study (Paper III) used parameters from a previous work [51], and a simulation response is presented in Fig. 3.2.

Table 3.1 Model parameter values used in Paper II & V.

Parameter	Value	Unit
ε_c	0.4	-
ε_p	0.6	-
$\mathscr{D}_{\text{app},\alpha}$	5.4×10^{-12}	m^2/s
$k_{\text{kin},\alpha}$	1×10^3	$(\text{m}^3/\text{mol})^{\nu_\alpha}\text{s}^{-1}$
ν_α	2.3	-
q_{max}	75.4	mol/m^3
$K_{eq,Sm}$	0.41	$(\text{mol}/\text{m}^3)^{\nu_\alpha - 1}$
$K_{eq,Eu}$	0.81	$(\text{mol}/\text{m}^3)^{\nu_\alpha - 1}$
$K_{eq,Gd}$	1.27	$(\text{mol}/\text{m}^3)^{\nu_\alpha - 1}$
$\dot{Q}$	0.5	ml/min
V_{mix}	0.1	ml
τ_{mix}	0.2	min

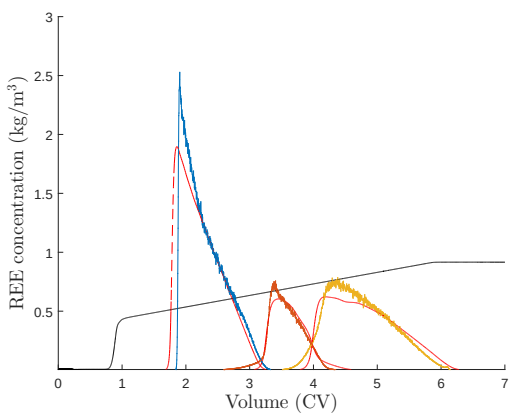

Figure 3.1 Model response chromatogram (red dashed lines) plotted against experimental data. The elution order is Sm, Eu and Gd. The unit for the nitric acid elution gradient (black dashed line) on the vertical axis is mole/litre.

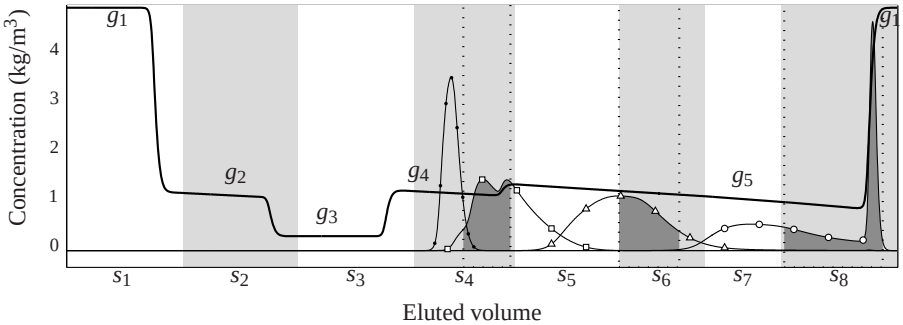

Figure 3.2 Simulation of two-column MCSGP with (− • −) Nd; (−□−) Sm; (−△−) Eu; (− ○ −) Gd and the nitric acid modifier (−). The chromatogram is formed by joining s_1 to s_8. Cut points for the pooling are seen as shaded peaks with dotted borders. The nitric acid gradient consists of five sections denoted as $g_1 - g_5$. Sm is scaled by a factor of 0.1.

4

Multi-objective optimization

4.1 Optimization

Optimization involves the selection of the best option from the available alternatives. For chemical process engineering, this means choosing the operating conditions that will produce the most lucrative outcome for the desired objective. This makes the definition of the objective a central part of the optimization process, as it decides the target for the optimization [5, 58]. The objective can for example be to maximize production rate and product quality, or minimize plant downtime. In the context of mathematical optimization, the objective is defined through the formulation of an objective function that depends on several variables that in turn can be divided into two groups; (*i*) decision variables and (*ii*) fixed parameters. The decision variables comprise the conditions that are being altered during the optimization, and the fixed parameters are kept constant. Finally, some constraints are normally introduced to make sure that the optimization results remain within a feasible region. In its general form [6, 7], the optimization problem can be formulated as:

$$
\begin{aligned}
\min_{\boldsymbol{u}} \quad & \boldsymbol{f}(\boldsymbol{u}) \\
\text{s.t.} \quad & 0 = \boldsymbol{F}\left(t, \dot{\boldsymbol{x}}, \boldsymbol{x}, \boldsymbol{w}, \boldsymbol{u}, \boldsymbol{p}\right), \\
& 0 = \boldsymbol{F}_0\left(t_0, \dot{\boldsymbol{x}}(t_0), \boldsymbol{x}(t_0), \boldsymbol{w}(t_0), \boldsymbol{u}(t_0), \boldsymbol{p}\right), \\
& \boldsymbol{y} = \boldsymbol{g}\left(\boldsymbol{x}, \boldsymbol{w}, \boldsymbol{u}, \boldsymbol{p}\right), \\
& 0 \leq \boldsymbol{C}_{ieq}\left(\dot{\boldsymbol{x}}, \boldsymbol{x}, \boldsymbol{w}, \boldsymbol{u}, \boldsymbol{p}\right), \\
& 0 = \boldsymbol{C}_{eq}\left(\dot{\boldsymbol{x}}, \boldsymbol{x}, \boldsymbol{w}, \boldsymbol{u}, \boldsymbol{p}\right), \\
& \boldsymbol{x}_{min} \leq \boldsymbol{x} \leq \boldsymbol{x}_{max}, \qquad \boldsymbol{w}_{min} \leq \boldsymbol{w} \leq \boldsymbol{w}_{max}, \\
& \boldsymbol{u}_{min} \leq \boldsymbol{u} \leq \boldsymbol{u}_{max}, \qquad \boldsymbol{x}(t_0) = \boldsymbol{x}_0,
\end{aligned}
\tag{4.1}
$$

where $\boldsymbol{f}$ denotes the objective function, $\boldsymbol{F}$ the differential algebraic equation (DAE) system, $\boldsymbol{u}$ the decision variables, $\boldsymbol{p}$ the model parameters, $\boldsymbol{x}$ the state variables, $\boldsymbol{w}$ the algebraic variables, $\boldsymbol{C}_{ieq}$ the inequality constraints, $\boldsymbol{C}_{eq}$ the equality constraints, $\boldsymbol{x}_0$ the initial state, and $\boldsymbol{g}$ the response function that governs the model output $\boldsymbol{y}$.

In the context of chromatography, the objective function regularly involves a target such as productivity and yield. The decision variables can include column load size, flow rates and modifier gradient settings, and finally, the fixed parameters normally comprise

column and particle dimensions. It should however be noted that depending on what the optimization is intended to achieve, the definition of the objective function and what is considered as a variable or a fixed parameter may change.

4.1.1 Experimental optimization study

A basic example of a process optimization can be illustrated by reviewing the experimental optimization study in Paper I, where the objective was to maximize the productivity. The decision variables consisted of the flow rate and the batch load size, the constraints were made out of product purity and yield requirements, and an estimation of optimal elution gradient settings were included as fixed parameters along with the configuration of the chromatography system. The objective function was in this case expressed as:

$$P_i = \frac{L_i Y_i}{t_c V_{col}}, \tag{4.2}$$

where P_i is the productivity for component i, the load L_i is defined as the product of the feed concentration of component i and the feed volume, t_c is the total cycle time and V_{col} is the total column volume. The yield, Y_i, of component i was defined as:

$$Y_i = \frac{c_{pool,i} V_{pool,i}}{L_i}, \tag{4.3}$$

where $c_{pool,i}$ is the product pool concentration and $V_{pool,i}$ is the product pool volume of component i. The inequality constraints were set to:

$$0.99 - X_i \leq 0, \qquad 0.80 - Y_i \leq 0,$$

where X_i denotes the product pool purity for component i.

Results from the flow rate and batch load size optimizations are given in Table 4.1 and 4.2, where it can be seen how the productivity changed when the flow rate and batch load were varied. The conclusions from the study were that a flow rate of 0.5 ml/min and a batch load of 150 μl gave a productivity close to the optimum. The study could have continued with several further experiments to try to pinpoint the optimal conditions, but turning to a model based optimization approach that considered additional objectives and decision variables was more appealing for several reasons. The experimental work consumed much resources which could be avoided by a model based approach. The number of needed experiments would grow as studies with varying elution gradients were needed due to that its impact on the system performance was expected to be significant. It was also found that productivity was not a sufficient objective on its own, and yield and pool concentration needed to be included as objectives with the intention of enabling use of the objective function for purposes such as a comprehensive production cost perspective. Therefore, it was decided to employ a model based multi-objective optimization method to further investigate the impact of batch load and elution gradient settings, and to formulate a general strategy for desirable operating points.

Table 4.1 Results from the flow rate experiments showing that with an increased flow rate, the yield decreases and the productivity increases until the yield becomes so low that it is detrimental to the productivity. This is accentuated for Eu. The highest productivity, with respect to the constraints, was achieved at a flow rate of 0.5 ml/min.

Flow rate (ml/min)	Prod ($kg/h\,m^3_{column}$)	Yield (%)	c_{pool} (kg/m^3)
0.25	0.66 Sm	99.7 Sm	0.64 Sm
	0.19 Eu	98.4 Eu	0.35 Eu
	0.41 Gd	99.6 Gd	0.46 Gd
0.50	1.24 Sm	99.6 Sm	0.78 Sm
	0.34 Eu	84.1 Eu	0.46 Eu
	0.84 Gd	97.2 Gd	0.34 Gd
0.75	2.34 Sm	72.5 Sm	0.96 Sm
	0.0 Eu	0.0 Eu	0.0 Eu
	1.52 Gd	75.9 Gd	0.46 Gd

Table 4.2 Results from the load experiments showing that with an increased batch load, the yield decreases and the productivity increases until the yield becomes so low that it negatively affects the productivity. The highest Eu productivity was achieved at 150 μl load.

Load (μl)	Prod ($kg/h\,m^3_{column}$)	Yield (%)	c_{pool} (kg/m^3)
150	1.32 Sm	99.9 Sm	0.55 Sm
	0.38 Eu	95.5 Eu	0.32 Eu
	0.81 Gd	99.0 Gd	0.35 Gd
180	1.24 Sm	99.6 Sm	0.78 Sm
	0.34 Eu	84.1 Eu	0.46 Eu
	0.84 Gd	97.2 Gd	0.34 Gd
200	1.45 Sm	98.0 Sm	0.83 Sm
	0.31 Eu	73.5 Eu	0.49 Eu
	0.91 Gd	95.9 Gd	0.46 Gd
220	1.48 Sm	96.7 Sm	1.09 Sm
	0.25 Eu	51.9 Eu	0.61 Eu
	0.99 Gd	91.4 Gd	0.41 Gd

4.2 Multi-objective optimization problem

The purpose of an multi-objective optimization is to produce a set of Pareto optimal solutions for the optimization problem. Pareto optimality implies a solution where an objective cannot be improved without decreasing another objective. The solution set will become a two-dimensional Pareto front when the optimization problem consists of two competing objectives, and three competing objectives will result in a Pareto surface. Adding further competing objectives will make the solution more complex and result in a less perceptible visualization, but the multi-objective optimization problem (MOP) formulation and optimization method presented here can readily be extended to produce such solutions. This work has considered the two competing objectives productivity and yield in Paper III-V, and Paper II also includes pool concentration as a third competing objective. The MOP for three competing objectives (Paper II) will be presented here, as it is the most complex scenario within this work.

The MOP formulation will begin by defining the competing objectives individually, and then combine these into a single objective by means of the weighted sum scalarization method [5, 17, 30, 41, 42]. The optimization problem for the chromatography system is then, in agreement with regular practice [60], cast in a bi-level framework. The upper level incorporates the impact of the decision variables, such as load and elution gradient slope, that governs the chromatogram, and the lower level constitutes the pooling strategy that decides the cut-times for the product pooling. The resulting MOP can be solved by using soft objective metrics as in [48], but the preferred approach in this work is to use firm objectives when evaluating the MOP.

4.2.1 Multi-objective optimization problem formulation

The column outlet concentration profile, $c_\alpha(t,z_f)$ where $\alpha \in \{\text{REE}\}$, is used for evaluation of the competing objective functions; yield, Y_α, productivity, P_α, and pool concentration, C_α, for the target component. The objective functions for the collected component, α, between the cut-times $[t_c,t_f]$ are defined as:

$$\delta_{\text{load},\alpha}\frac{\mathrm{d}Y_\alpha}{\mathrm{d}t} = c_\alpha(t,z_f)v_{\text{int}}A_c\Pi(t,t_c,t_f), \tag{4.4}$$

$$\frac{\mathrm{d}P_\alpha}{\mathrm{d}t} = \frac{1}{V_c}\frac{1}{(t_f+t_r)}\delta_{\text{load},\alpha}\frac{\mathrm{d}Y_\alpha}{\mathrm{d}t}, \tag{4.5}$$

$$\frac{\mathrm{d}C_\alpha}{\mathrm{d}t} = \delta_{\text{load},\alpha}\frac{\mathrm{d}Y_\alpha}{\mathrm{d}t}\frac{1}{v_{\text{int}}A_c}\frac{1}{(t_f-t_c)}, \tag{4.6}$$

where $\delta_{\text{load},\alpha} = c_{\text{load},\alpha}v_{\text{int}}A_c\Delta t_{\text{load}}$ is the total amount of injected sample, A_c and V_c the column cross-sectional area and volume, and $t_r = 2V_c\dot{Q}^{-1}$ the regeneration and re-equilibration time following the final cut-time. The main goal becomes to determine the optimal decision variables (such as elution gradient, u, batch load, $\delta_{\text{load},\alpha}$, and pooling cut-times, $[t_c,t_f]$) that maximizes $Y_\alpha(t_f)$, $P_\alpha(t_f)$ and $C_\alpha(t_f)$, while fulfilling the target component purity constraint given by:

$$X_\alpha(t_f) = \frac{\delta_{\text{load},\alpha}Y_\alpha(t_f)}{\sum\limits_{b\in\{\text{REEs}\}}\delta_{\text{load},b}Y_b(t_f)}, \tag{4.7}$$

where the numerator is the captured amount of the target component in $[t_c,t_f]$ and the denominator represents the total amount of captured components. The weighted sum scalar-

ization method combines the objectives in Eqs. (4.4–4.6) to a single objective with the weights ω_i, defined as; $\sum_{i=1}^{3}\omega_i = 1$, and $\omega_i \in [0,1]$. In addition to this, each individual objective is also normalized with respect to its maximum single objective value. The decision variables determine the trajectories $\boldsymbol{x} = (c_\alpha(t,z_k), c_S(t,z_k), c_{\mathrm{mix},S}(t), q_\alpha(t,z_k), P_\alpha(t), Y_\alpha(t), X_\alpha(t))$. The resulting optimization problem can then be set in the framework for *min–min optimal control*:

$$\text{min.} \quad -\left(\omega_1 \int_{t_0}^{t_f} \frac{\mathrm{d}P_\alpha}{\mathrm{d}t}\mathrm{d}t + \omega_2 \int_{t_0}^{t_f} \frac{\mathrm{d}Y_\alpha}{\mathrm{d}t}\mathrm{d}t + \omega_3 \int_{t_0}^{t_f} \frac{\mathrm{d}C_\alpha}{\mathrm{d}t}\mathrm{d}t\right), \tag{4.8a}$$

$$\text{w.r.t.} \quad \boldsymbol{p} = (\Delta t_{\mathrm{load}}, u_0, u_f) \in \mathbb{R}^3,$$

$$\text{s.t.} \quad \boldsymbol{p}_L \leq \boldsymbol{p} \leq \boldsymbol{p}_U, \tag{4.8b}$$

$$(\boldsymbol{x}, t_c, t_f) = \arg\min. -\left(\omega_1 \int_{t_0}^{t_f} \frac{\mathrm{d}P_\alpha}{\mathrm{d}t}\mathrm{d}t + \omega_2 \int_{t_0}^{t_f} \frac{\mathrm{d}Y_\alpha}{\mathrm{d}t}\mathrm{d}t + \omega_3 \int_{t_0}^{t_f} \frac{\mathrm{d}C_\alpha}{\mathrm{d}t}\mathrm{d}t\right), \tag{4.8c}$$

$$\text{w.r.t.} \quad (t_c, t_f) \in \mathbb{R}^2,$$

$$\text{s.t.} \quad \dot{\boldsymbol{x}} = \boldsymbol{F}\left(t, \boldsymbol{x}(t), t_c, t_f, \boldsymbol{p}\right), \quad \boldsymbol{x}(t_0) = \boldsymbol{x}_0, \tag{4.8d}$$

$$X_{\alpha,L} - X_\alpha(t_f) \leq 0, \tag{4.8e}$$

$$t_{c,L} \leq t_c \leq t_{c,U}, \qquad t_{f,L} \leq t_f \leq t_{f,U}, \tag{4.8f}$$

$$\forall t \in [t_0, t_f], \qquad \forall z \in [z_0, z_f].$$

A decomposition strategy was adopted to transform the MOP into two levels: (i) the upper-level static optimization problem given by Eqs. (4.8a-4.8b) with respect to $\boldsymbol{p}$, and (ii) the lower-level optimization problem given by Eqs. (4.8c-4.8f) and constrained by the ODE system, $\boldsymbol{F}$, governed by Eqs. (3.1,3.2,3.5,4.4-4.7).

4.3 Optimization methods

Generally, it is beneficial to carry out a pre-optimization step to provide with an early visualization of the MOP dynamics and near optimum starting points for the optimization decision variables. This can be produced by evaluating model responses from a latin hyper cube sampling (LHS) of several decision variable sets.

Solutions to a MOP can be found through genetic algorithms as in Paper III and IV. Genetic algorithms are search methods that find the global optimum for an optimization problem, and they are suitable for solving multi-objective optimizations [5, 63]. The starting point for a genetic algorithm is to create an initial population where each individual has a unique set of decision variable values. The system response from each individual is then evaluated and a new population is created from combinations and permutations of the old individuals. The two populations are then compared and the individuals with the best objective values are used for the next population generation. This is repeated until individuals with improved objective values, given a certain tolerance, cease to occur.

Solutions to a MOP can also be found by employing gradient based methods that utilize information from the objective function gradient, with respect to changes in the decision variables, to assess the search direction for finding the optima [6]. The MOP is then converted into a series of single-objective optimization problems by means of a weighted sums method, and the solutions are consolidated into a Pareto optimal set as in Paper II. In this case, MATLABs *fmincon* function with a sequential quadratic programming algorithm, the

BFGS formula for updating the approximation of the Hessian matrix, and central differences to estimate the gradient of the objective function was utilized. The weighted sums method was implemented by creating a set of values for the weight of the first competing objective, ω_1, spanning between $\omega_1 \in [0,1]$. For each of the fixed weights, a 2-dimensional Pareto front was created between the two remaining competing objectives with weights defined as $\sum_{i=2}^{3} \omega_i = 1 - \omega_1$, and $\omega_i \in [0, 1 - \omega_1]$. When all the weights in the ω_1 set had been handled, the same procedure was repeated for the remaining competing objectives by changing the index of the fixed weight to ω_2 and finally ω_3. This procedure results in a sampling of the 3-dimensional Pareto surface for the MOP given by Eq. (4.8), where each generated Pareto front can be regarded as a two-dimensional projection of the final Pareto surface.

4.4 Optimization results

4.4.1 Tri-objective batch separation

In Paper II, a tri-objective optimization with respect to productivity, yield and pool concentration was conducted for the separation of the middle REEs samarium (Sm), europium (Eu) and gadolinium (Gd). The optimization method was utilized to find the process objective space as well as the corresponding decision variable space. The latter was in turn utilized to formulate a general strategy for achieving desirable operation points.

4.4.1.1 Finding the objective space

A pre-optimization step was carried out by producing a LHS of 10.000 different decision variable sets via MATLAB's *lhsdesign* function. The chromatography model response from these sets were evaluated and utilized to produce an early visualization of the optimization problem dynamics as shown in Figure 4.1.

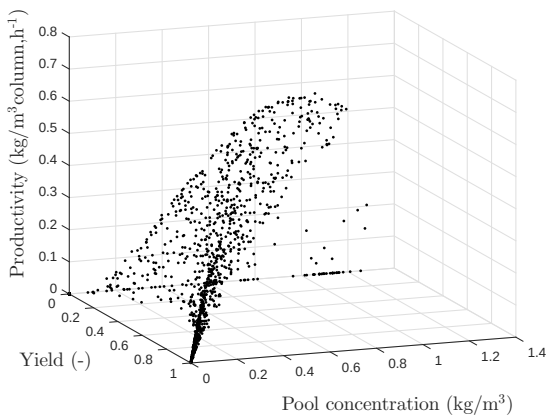

Figure 4.1 Outcome from a LHS with 10.000 unique sets of decision variables, where each resulting chromatogram has been evaluated according to the lower-level optimization problem. The LHS gives an early indication of what can be expected from the multi-objective optimization, and provides with viable starting points for the same.

The LHS response sets provided with near optimum starting points for the optimization, which resulted in a sampling of the 3-dimensional Pareto surface as shown in Figure 4.2(d). Figure 4.2(a)-(c) show the Pareto fronts where only the outermost points are Pareto optimal in a 2-dimensional competing objective sense, and the other points are projections from the 3-dimensional Pareto surface onto the 2-dimensional objective space. It is noteworthy to mention that it would require several thousand experiments to obtain this sampling of the Pareto surface.

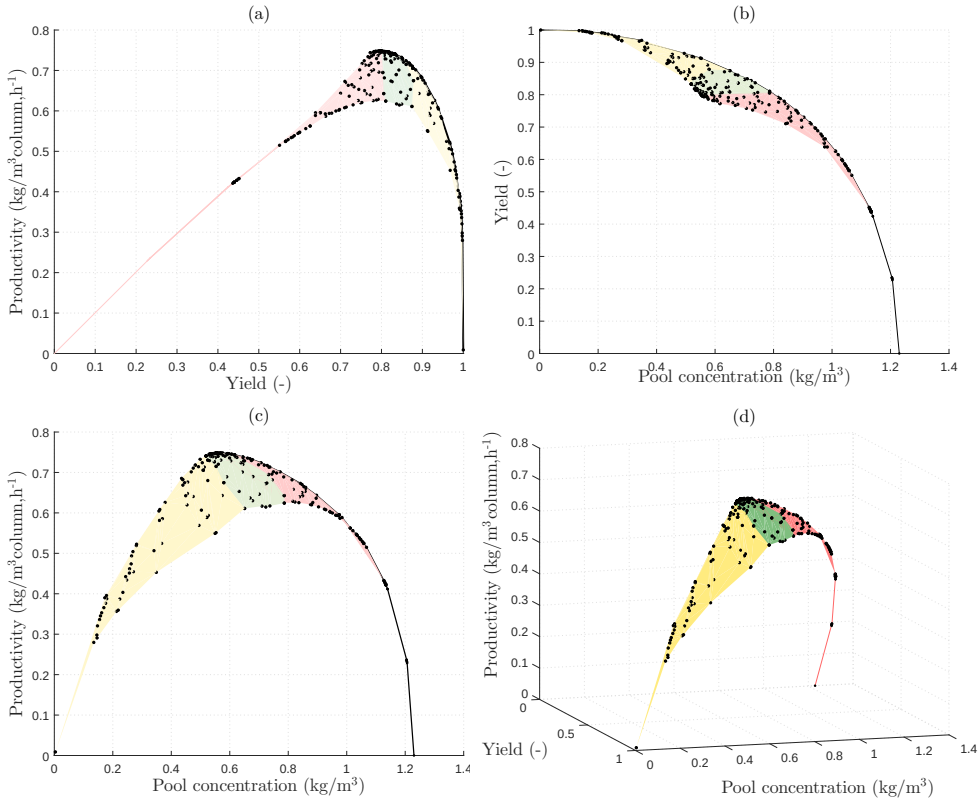

Figure 4.2 (a) Pareto front between productivity and yield. (b) Pareto front between yield and pool concentration. (c) Pareto front between productivity and pool concentration. (d) Pareto surface between all competing objectives. The resulting Pareto fronts in (a)-(c) are located to the right and are indicated with solid black lines. The Pareto surface (d) is divided into three objective space regions that are highlighted in green (recommended), yellow (plausible) and red (undesirable). These regions are also shaded accordingly in the Pareto front figures (a)-(c).

The optimal single objective values were a productivity of 0.75 kg $\mathrm{Eu/m^3_{column}, h^{-1}}$, 100% yield, and a pool concentration of 1.23 kg $\mathrm{Eu/m^3}$. Chromatograms for the operation points that correspond to these values are shown in Figure 4.3(a)-(c), and Figure 4.3(d) shows a chromatogram from the centre of the recommended objective space.

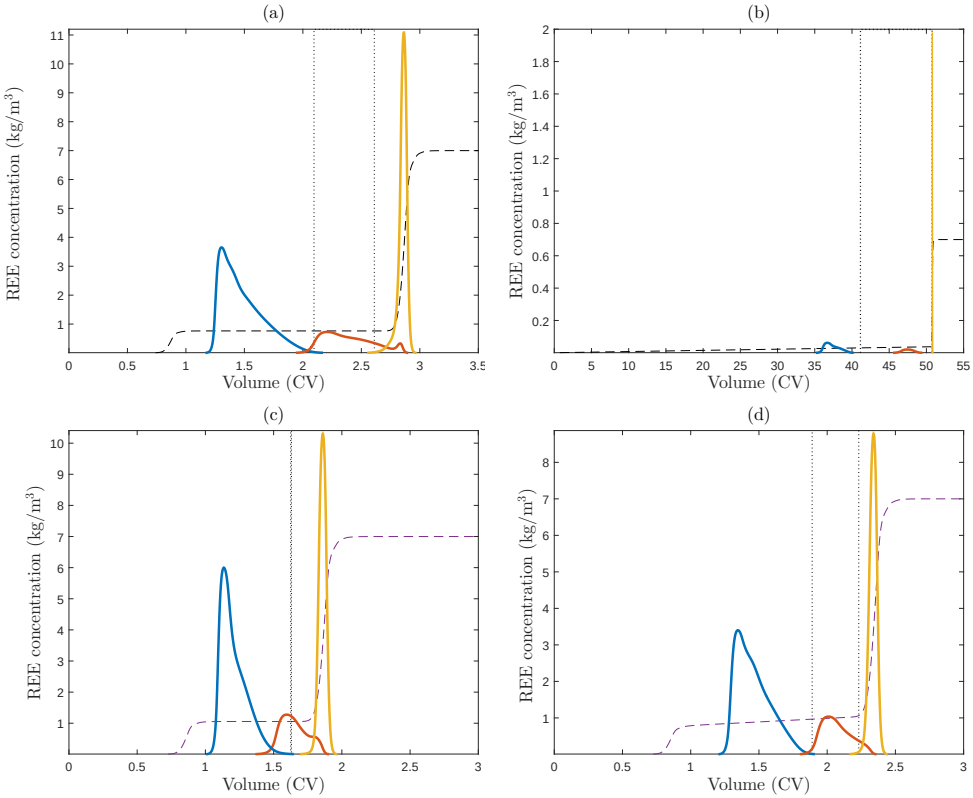

Figure 4.3 Chromatograms for different objective weights. The pooling cut times are indicated by the dotted lines, and the elution order is Sm, Eu and Gd. The unit for the nitric acid elution gradient (black dashed line) on the vertical axis is mole/litre. (a) Chromatogram for maximum productivity. (b) Chromatogram for maximum yield, where the final cut time is directly before the Gd peak. (c) Chromatogram for maximum pool concentration, where the cut times appear to coincide due to the small pooling volume. (d) Chromatogram from the recommended Pareto surface.

4.4.1.2 Strategy for achieving desirable operation points

The optimization procedure enabled a mapping of the optimization variables impact on each single objective and this facilitated to formulate a general strategy for achieving desirable operation points. The mapping is visualized in Fig. 4.4, where optimization variables are plotted against the single objective values. The results show that when the over-all objective is leaning towards maximizing yield, a small batch load and a long elution gradient are favoured since this allows for baseline separation. The initial acid concentration of the elution gradient is not a major concern until it approaches the upper boundary and separation becomes difficult, which is indicated by the drastic yield drop. Large pooling volumes will also be favoured since it allows for collecting as much of the load as possible.

When the objective leans more towards maximizing productivity; a larger batch load is favoured since it increases the product throughput per cycle, an elution gradient with fairly low initial acid concentration and a steeper slope is favoured to allow for a better separation between the first eluting component, Sm, and the middle eluting component Eu. A large pooling volume is favoured since it allows for more collected product.

When a high pool concentration is desired; a large load is favoured to increase the total product content in the pool, a short elution gradient with a high initial acid concentration is favoured to avoid pool dilution, and the pooling volume is set as small as possible at the concentration profile peak while still fulfilling the purity constraint.

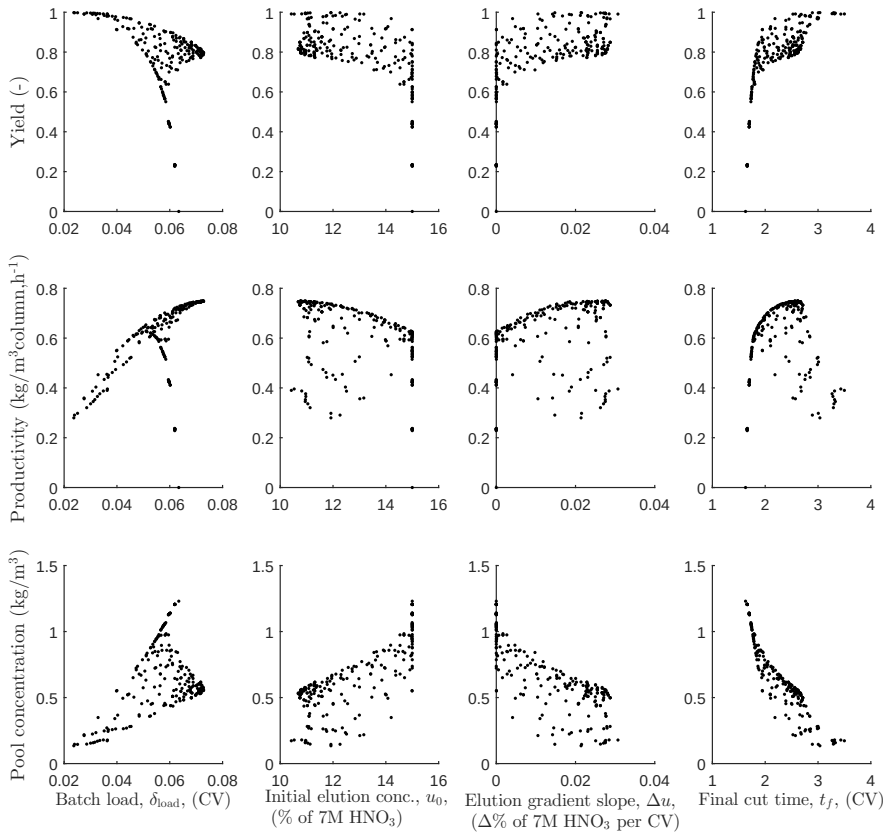

Figure 4.4 Decision variables plotted against individual objective values. The plots show the variable impact on each single objective and are used for deciding a desirable operation point strategy.

4.4.2 Comparison of MCSGP and batch separation

A performance comparison between twin-column MCSGP and batch separation of the middle REEs was conducted in Paper III. Two bi-objective optimizations were conducted; (*i*) specific productivity vs. yield and (*ii*) productivity vs. yield. The resulting Pareto fronts are illustrated in Figure 4.5, where it can be seen that the MCSGP Pareto solutions achieved higher values in the whole range compared to the batch separation, and the favouring of MCSGP over batch processes is also supported by [38]. It should be noted that the significantly lower solvent consumption for MCSGP could be achieved due to a more efficient solvent utilization through internal recycling.

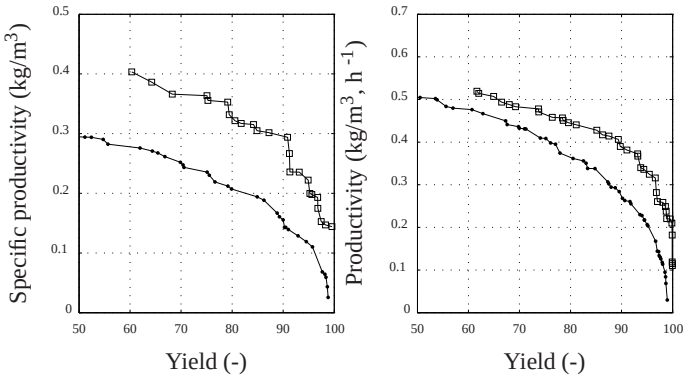

Figure 4.5 Optimal Pareto solutions for the batch (−●−) and MCSGP (−□−) cases. (left) Specific productivity vs. yield. (right) Productivity vs. yield.

4.4.3 Thulium purification

The purification of thulium (Tm) in a heavy REE stream from a liquid-liquid extraction step was studied in Paper IV. The stream held a very high ytterbium (Y) content, which exacerbated the collection of a pure thulium pool due to displacement effects. The resulting Pareto front is given in Figure 4.6, where it can be seen that a Tm productivity ranging between 0.1-0.45 $\mathrm{kg/m^3_{column}, h^{-1}}$ for yields between 73-99% was achieved under a purity constraint of 0.99.

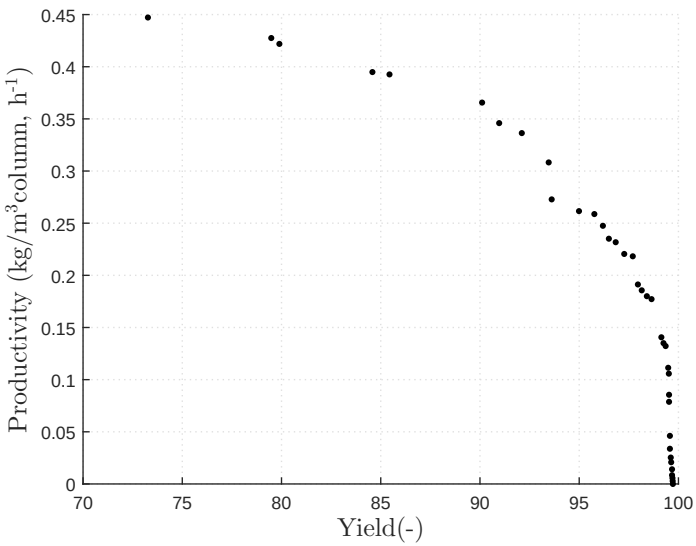

Figure 4.6 Productivity vs. Yield Pareto front from the Thulium purification optimization.

5

Robust multi-objective optimization

5.1 Robust optimization

The optimization of a chromatography system is ordinarily cast in a bi-level framework [61] with (*i*) the upper level that administer the effects of the decision variables, such as load and elution gradient, that governs the chromatogram, and (*ii*) the lower level that establishes the pooling strategy for deciding the product pooling cut-times. A multi-objective optimization method, as described in Chapter 4, is needed when competing optimization objectives, such as productivity and yield, are considered. However, the nominal solution for a MOP is often not robust and this implies that even small process disturbances may cause process failure, *i.e.* the purity requirement is not met, for an operating point in the nominal Pareto set.

Robustness can be achieved by transforming the MOP into its robust counterpart problem [4, 47] with robustness as an additional conflicting objective[29, 41]. Robustness will become a conflicting objective since an increased robustness will decrease the process performance compared to the nominal soultion. The process uncertainties can be considered by a deterministic approach through linearization of the uncertainty set [29, 41], a stochastic approach [15], or a worst case problem approach [47, 50] where the robust design problem is formulated with only the vertices of the uncertainty region that has the most negative impact on the objective. There is also the option to achieve robustness by focusing on the product pooling cut point stragey as in [19, 32], or applying a variable pooling cut time control strategy as described in [65].

The preferred robust optimization method used in this work includes transformation of the MOP into its robust counterpart problem, and utilization of a stochastic method to obtain model responses of the introduced process disturbances. The stochastic approach has the benefit of being more straightforward compared to deterministic approaches, at the expense of an increased demand of computation power. The increased computation power demand was accommodated for by using a parallel computing methodology as described in [1, 2].

5.2 Robust counterpart problem formulation

Here, the robust counterpart problem formulation is presented in the context of separating the intermediately eluting component, Eu, from a mix of middle REEs as described in Paper V. The robust counterpart problem is extended from the MOP as defined in Eq. (4.8), though the competing objectives are limited to only consider productivity and yield.

In order to formulate a robust counterpart of Eq. (4.8), a set of bounded distributed disturbances, $\tilde{\boldsymbol{p}}$, on the free operating parameters, $\boldsymbol{p}$ (i.e $\Delta t_{\text{load}}, u_0$ and u_f) is considered, and $\tilde{X}_{\text{Eu}}$ is defined as the cumulative purity distribution of the model responses that are produced from the disturbance set $\tilde{\boldsymbol{p}}$. A purity constraint back off term , X_{BF}, is introduced in order to make the purity constraint robust with respect to the disturbances. The back off term can essentially be seen as a safety margin that amplifies the purity inequality constraint in Eq. (4.8e) so that the purity requirement, $X_{\text{Eu,L}}$, still can be met for the considered set of bounded disturbances. The success rate is defined as the fraction of batches in the disturbance set that fulfil the purity requirement, $X_{\text{Eu,L}}$, and $\Phi_{X_{\text{Eu}}}$ signifies the desired success rate. The following robust counterpart of Eq. (4.8) is then given by:

$$\min. \quad \int_{-\infty}^{X_{\text{Eu},L}+X_{\text{BF}}} \tilde{X}_{\text{Eu}} \mathrm{d}X_{\text{Eu}} - \Phi_{X_{\text{Eu}}}, \tag{5.1a}$$

$$\text{w.r.t.} \quad X_{\text{BF}},$$

$$\text{s.t.} \quad \dot{\tilde{\boldsymbol{x}}} = \tilde{\boldsymbol{F}}\left(t, \boldsymbol{x}(t), t_c, t_f, \tilde{\boldsymbol{p}}\right), \tag{5.1b}$$

$$\tilde{\boldsymbol{p}} \sim \mathcal{N}\left(\boldsymbol{p}, \sigma_{\boldsymbol{p}}^2\right), \tag{5.1c}$$

$$\boldsymbol{p} = \arg\min. \quad -\left(\omega \int_{t_0}^{t_f} \frac{\mathrm{d}P_{\text{Eu}}}{\mathrm{d}t}\mathrm{d}t + (1-\omega)\int_{t_0}^{t_f} \frac{\mathrm{d}Y_{\text{Eu}}}{\mathrm{d}t}\mathrm{d}t\right), \tag{5.1d}$$

$$\text{w.r.t.} \quad \boldsymbol{p} = (\Delta t_{\text{load}}, u_0, u_f) \in \mathbb{R}^3,$$

$$\text{s.t.} \quad \boldsymbol{p}_L \leq \boldsymbol{p} \leq \boldsymbol{p}_U, \tag{5.1e}$$

$$\left(\boldsymbol{x}, t_c, t_f\right) = \arg\min. -\left(\omega \int_{t_0}^{t_f} \frac{\mathrm{d}P_{\text{Eu}}}{\mathrm{d}t}\mathrm{d}t + (1-\omega)\int_{t_0}^{t_f} \frac{\mathrm{d}Y_{\text{Eu}}}{\mathrm{d}t}\mathrm{d}t\right), \tag{5.1f}$$

$$\text{w.r.t.} \quad (\boldsymbol{t}_c, t_f) \in \mathbb{R}^2,$$

$$\text{s.t.} \quad \dot{\boldsymbol{x}} = \boldsymbol{F}\left(t, \boldsymbol{x}(t), t_c, t_f, \boldsymbol{p}\right), \quad \boldsymbol{x}(t_0) = \boldsymbol{x}_0, \tag{5.1g}$$

$$\left(X_{\text{Eu},L} + X_{\text{BF}}\right) - X_{\text{Eu}}(t_f) \leq 0, \tag{5.1h}$$

$$t_{c,L} \leq t_c \leq t_{c,U}, \qquad t_{f,L} \leq t_f \leq t_{f,U}, \tag{5.1i}$$

$$\forall t \in [t_0, t_f], \qquad \forall z \in [z_0, z_f].$$

A decomposition strategy is adopted to transform the robust MOP into three levels: (i) the upper-level optimization problem given by Eqs. (5.1a-5.1c) with respect to X_{BF}, (ii) the mid-level optimization problem given by Eqs. (5.1d-5.1e) with respect to $\boldsymbol{p}$, and (iii) the lower-level optimization problem given by Eqs. (5.1f-5.1i) and constrained by the ODE system, $\boldsymbol{F}$, governed by Eqs. (3.1,3.2,3.5,4.4-4.7). Essentially, Eq. (5.1) can be solved by using the simulated system response, $\tilde{\boldsymbol{x}}$, for an uncertainty set of the free operating parameters, $\tilde{\boldsymbol{p}}$, to evaluate the cumulative distribution function of $\tilde{X}_{\text{Eu}}$. The back off term, X_{BF}, in the purity inequality constraint, Eq. (5.1h), can then be incrementally increased to gain

more successful batches in $\tilde{X}_{\mathrm{Eu}}$, and thereby achieving a more robust process. This procedure can then be repeated iteratively until Eq. (5.1a) is fulfilled, at which point Eq. (5.1) is considered to be solved.

5.3 Robust optimization method

As a first step, the nominal and non-robust Pareto front was obtained by solving the MOP as defined in Eq. (4.8). This was carried out through MATLAB's *fmincon* function with a sequential quadratic programming algorithm, the BFGS formula for updating the approximation of the Hessian matrix, and central differences to estimate the gradient of the objective function and constraint functions. Then an uncertainty set, $\tilde{\boldsymbol{p}}$, with a normal distribution, assuming no covariance between the free operating parameters $\boldsymbol{p}$, a standard deviation σ, and sampling size of 10.000 was obtained via MATLAB's *lhsnorm* function. The uncertainty set was applied to the investigated operating points on the nominal Pareto front, and the model responses were used to evaluate the cumulative purity distribution, $\tilde{X}_{\mathrm{Eu}}$, of the uncertainty set.

Then, an initial investigation of the back off term's impact on $\tilde{X}_{\mathrm{Eu}}$ was conducted by creating new Pareto fronts with an incrementally increased back-off and observing how $\tilde{X}_{\mathrm{Eu}}$ changes when $\tilde{\boldsymbol{p}}$ is applied to the investigated points on the new Pareto fronts. At this stage, it is of particular interest to investigate how the fraction of batches that fulfil the purity requirement in the perturbed set, changes with an increased back off. This provides an estimate of the required back-off to meet a certain success rate for a given purity constraint.

The required back off for a given point on the nominal Pareto front was obtained by applying MATLAB's *fminbnd* function on the upper level of the robust counterpart problem in Eq. (5.1), with suitable boundaries obtained from the previous back off investigation. The mid- and lower-level optimization problems in Eq. (5.1) were solved by MATLAB's *fmincon* function with a sequential quadratic programming algorithm, the BFGS formula for updating the approximation of the Hessian matrix, and central differences to estimate the gradient of the objective function and constraints. The procedure comprises an evaluation of the cumulative distribution function of $\tilde{X}_{\mathrm{Eu}}$ based on $\tilde{\boldsymbol{x}}$ and $\tilde{\boldsymbol{p}}$, as obtained from the mid- and lower-level optimization problem for a given initial X_{BF}. X_{BF} is then varied for the upper level optimization problem through MATLAB's *fminbnd* function, resulting in new $\tilde{\mathbf{x}}$, $\tilde{\boldsymbol{p}}$ and cumulative distribution functions of $\tilde{X}_{\mathrm{Eu}}$ to be evaluated. This continues until a X_{BF} that produces a cumulative distribution function of $\tilde{X}_{\mathrm{Eu}}$ corresponding to the desired success rate $\Phi_{X_{\mathrm{Eu}}}$ is obtained.

5.4 Results from robust multi-objective optimization

In Paper V, a robust bi-objective optimization with respect to productivity and yield was conducted for the separation of the middle REEs samarium (Sm), europium (Eu) and gadolinium (Gd). The perturbed process parameters were the injected load concentration, $c_{\mathrm{load},\alpha}$, and the modifier concentration in the upstream mixing tank, $c_{\mathrm{mix},S}$. The robust optimizations of the studied system were carried out for a product purity requirement, $X_{\mathrm{Eu,L}}$, of 0.95 and 0.99 respectively, and the target success rate, $\Phi_{X_{\mathrm{Eu}}}$, was set to 0.95.

An early investigation showed that the system is very un-robust, as a uncertainty set standard deviation, σ, exceeding 0.01 did not result in achieving robust Pareto sets with

respect to the desired $\Phi_{X_{\mathrm{Eu}}}$ target. The low robustness of the system can be explained by that the studied elements are extremely similar in both chemical and physical properties, resulting in a minute separation selectivity which in turn makes the separation very difficult and unforgiving towards process perturbations.

5.4.1 Initial robustness investigation for an increased back off

The nominal un-robust Pareto fronts are presented by the outermost fronts in Fig. 5.1, and it can be seen how the Pareto front decreases with an increased back off on the purity requirement for the studied Pareto points with different objective weights, ω.

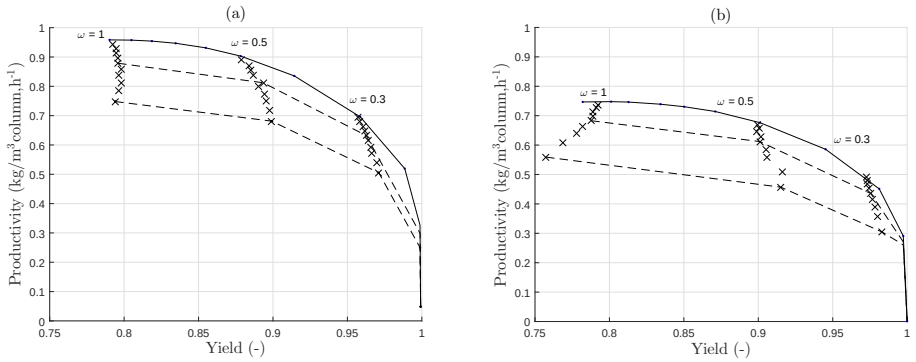

Figure 5.1 The nominal Pareto fronts are presented by the solid lines for a purity requirement of 0.95 in (a) and 0.99 in (b). The cross marks indicate how a Pareto point, with the weight ω, changes with an increased back off. The dashed lines indicate the Pareto front outlines for an increasing back off, and it can be seen that the Pareto front decreases as the back off is increased.

Fig. 5.2 shows how the success rate, $\Phi_{X_{\mathrm{Eu}}}$, for the investigated points on the nominal Pareto front increases with an increased back off. The figure provides with an estimation of the required back off to achieve the desired success rate for a given disturbance set, and it can be seen that an objective leaning more towards yield (*i.e.* ω decreases) results in a lower success rate for a given back off.

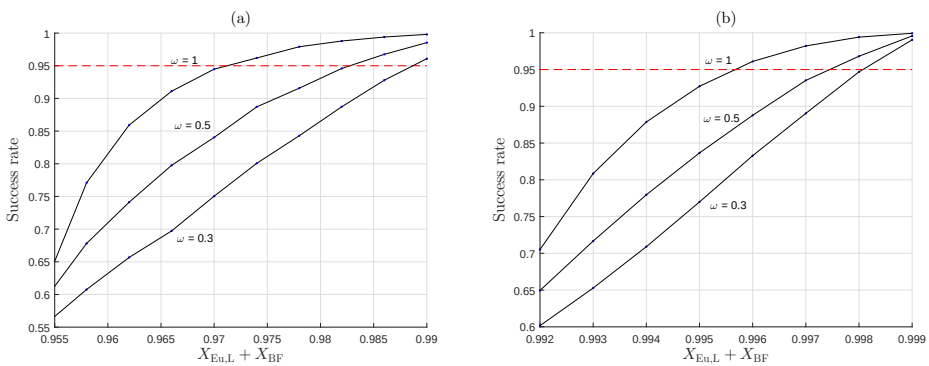

Figure 5.2 Results from the investigation of how the success rate increases with an increased back off for a purity requirement of 0.95 in (a) and 0.99 in (b). The dashed line indicates the target success rate, $\Phi_{X_{\mathrm{Eu}}}$, and helps to provide an initial estimation of the required back off, X_{BF}, for a Pareto point with the objective weight ω.

It is somewhat counter intuitive that the success rate should decrease with an increased objective weight for yield, since a higher yield typically is associated with an increased peak separation which in turn should result in an increased robustness. The decrease of robustness can be explained by observing how the decision variables change with an increased back off for the 0.95 purity requirement case in Fig. 5.3, where the pooling cut-time trends become very interesting.

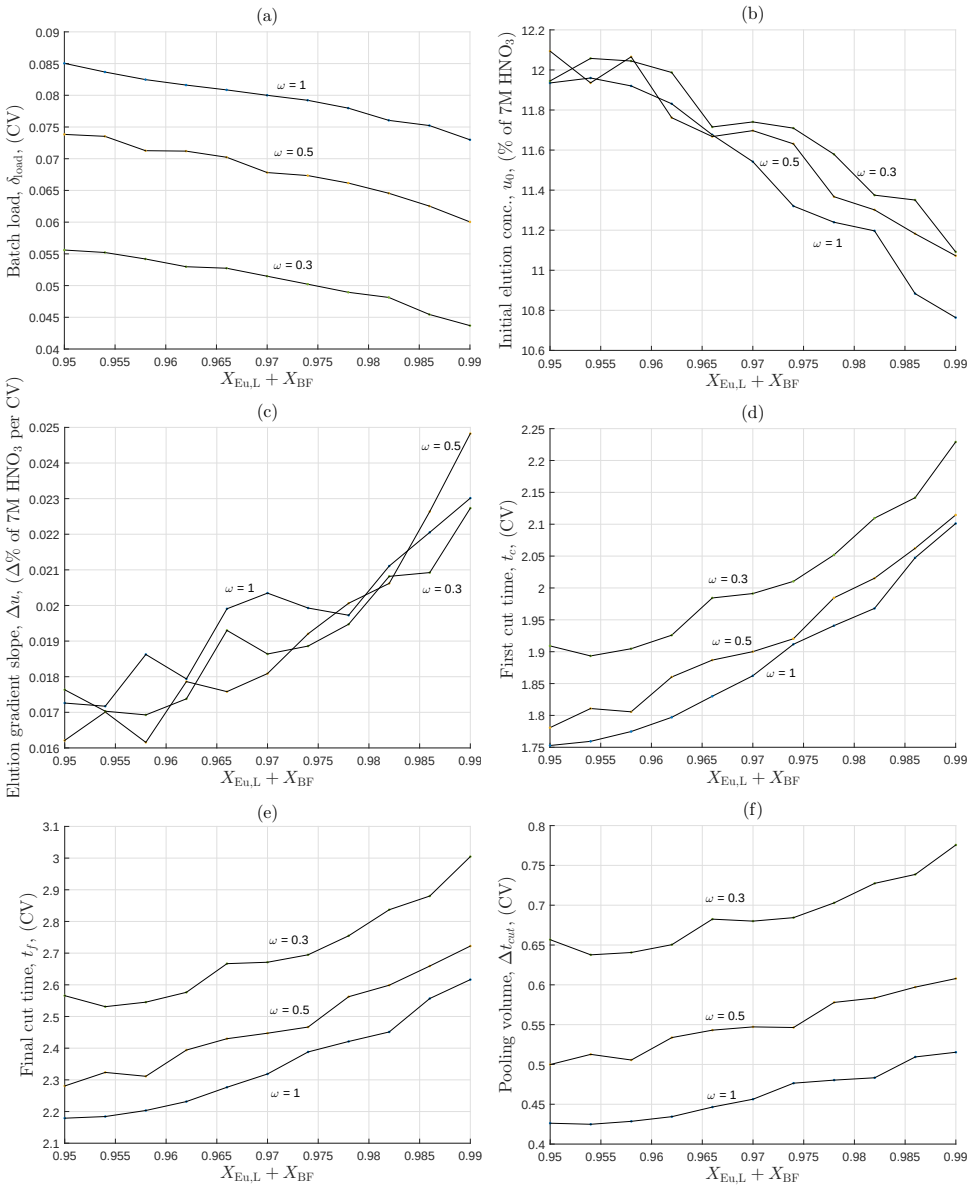

Figure 5.3 Plots of decision variable changes due to an increasing back off for Pareto points with different objective weights, ω, and a purity requirement of 0.95. (a) Batch load, (b) Initial elution concentration, (c) Elution gradient slope, (d) First cut time, (e) Final cut time, (f) Pooling volume.

The decision variable trends in Fig. 5.3 show that the initial elution concentration and elution gradient slope are quite similar as long as productivity is a part of the weighted objective. However, a higher productivity is favoured by a larger batch load, a pooling horizon occurring earlier in the chromatogram (*i.e.* first and last pooling cuts occur earlier) and a smaller pooling volume. The increased batch load is reasonable since it will allow for a higher productivity due to an increased throughput. The early first cut comes from that a higher batch load will capacitate the elements to start eluting earlier. The earlier final cut makes the cycle time shorter, which is favourable for productivity, but it is also a trade off in terms of decreased yield. This has the implication of that a high objective weight on productivity will result in pooling cut times occurring closer to the Eu elution peak centre and farther away from the neighbouring peaks. When a higher yield is desired, the pooling horizon will increase in order to capture more of the target molecules, and this will move the pooling close to, and even into, the neighbouring elution peaks as long as the purity requirement is met. For this reason, a higher weight on yield will demand a higher back off on purity in order to meet the desired success rate. This is due to that when a perturbation is introduced, the neighbouring peaks may move closer to, and even intrude, the pooling horizon, and a higher purity requirement will move the pooling cut times farther away from the neighbouring peaks. The farther away the cut times are from the neighbouring peaks in the nominal case, the higher disturbance can be tolerated since there is more room available for the neighbouring peaks to move before they impact the purity of the target peak. This is illustrated in Fig. 5.4 where a case with high productivity (smaller pooling horizon) and a case with high yield (larger pooling horizon) are presented, and it can be observed how the introduced process disturbances make the neighbouring peaks creep into the pooling horizon to a larger extent for the high yield case.

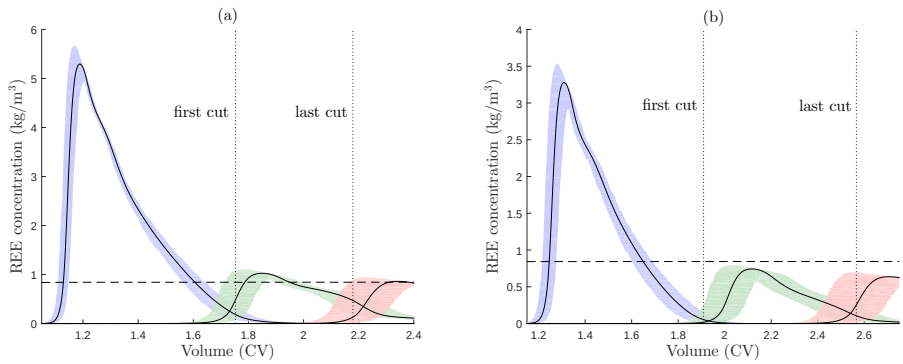

Figure 5.4 Sections of chromatograms with focus on the collection of the Eu product pool. The purity requirement, X_{Eu}, was set to 0.95 for the productivity objective weights ω =1 (a) and ω =0.3 (b). The pooling cut times are indicated by the dotted lines, and the elution order is Sm, Eu and Gd. The unit for the nitric acid elution gradient (black dashed line) on the vertical axis is mol/l. The shaded areas indicate the span of concentration profile variations due to process disturbances with σ = 0.01, and the solid black lines indicate the concentration profiles for the nominal case. The chromatograms demonstrate that an operation point with a higher objective weight for productivity (a), is more robust than an operation point with a lower weight (b). This can be seen by observing how the larger pooling horizon in (b) allows for more collection of the neighbouring elements when disturbances are introduced, and thereby causing an increased number of batches with failed purity requirement. This is particularly noticeable for the Gd peak which intrudes the collected pool to a larger extent when process disturbances are introduced in (b).

5.4.2 Robust Pareto fronts and benchmarking with an alternative robustness method

The robust Pareto fronts produced by the presented method are given in Fig. 5.5 along with the nominal un-robust Pareto front and a front produced by an alternative robust optimization method as presented in [19].

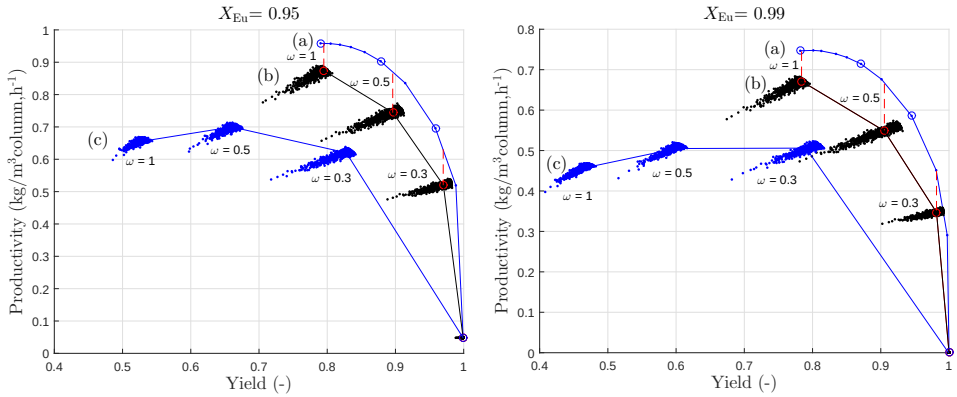

Figure 5.5 Pareto fronts resulting from the optimizations with a purity requirement of 0.95 (left) and 0.99 (right). (a) indicates the nominal Pareto front, (b) the robust Pareto front according to the presented method and (c) the robust front from an alternative cut-time focused method. The dots indicate the system response of the distributed uncertainty set associated with the respective Pareto points. The red dashed lines indicate the loss of productivity for a given yield when robustifying the nominal Pareto front according to the presented method.

The alternative method focuses on the nominal Pareto front and optimizes the pooling time horizon for each investigated point on the front so that the purity requirement is met for a given uncertainty set. The main difference is that the method in this work will find new optimal operation points by changing the free operating parameters, and achieve robustness by increasing the purity requirement back off for each point on the Pareto front, whereas the alternative method keeps the decision variables from the nominal Pareto front intact, with the exception of the cut-times that are optimized to find a fixed pooling time horizon that will fulfil the purity requirement for the entire uncertainty set. It should be noted that both methods provide with robust operating points that handle the given process disturbances satisfactorily. However, the presented method should be favoured since it produces a robust Pareto front with higher objective values compared to the alternative method, which implies that the cut-time focused method should be considered more restrictive. Further, the alternative method generates operating points that cannot be considered Pareto optimal, which is the case for the points with $\omega = 1$ on front (c), and as mentioned in [18], these points should be disregarded.

Applying robustness to a point on the nominal Pareto front with a given ω will result in a change of both productivity and yield, and this makes the evaluation of performance loss when introducing robustness slightly ambiguous. In order to resolve this, the productivity for a given yield on the nominal Pareto front is compared to the productivity on the robust Pareto front given the same yield, as indicated by red dashed lines in Fig. 5.5. Here, a productivity loss in the range of 10-20% was observed when robustness was accounted for, though it should be mentioned that the loss of productivity can be decreased by applying a variable pooling cut time control strategy as described in [65].

6

Conclusion

6.1 Summarizing conclusions

It has experimentally been shown that it is possible to achieve chromatographic separation of REEs, and process performance data for the separation of middle and heavy REE mixtures has been provided. Further, model based optimization methods have been presented and implemented for both batch and continuous chromatography. The optimizations have shown that a continuous two-column MCSGP process can outperform a batch process, though it should be mentioned that a batch process might be preferred due to a less demanding system configuration and operation scheme.

The optimization studies have not only provided expected process performance data and limitations, but also given insights about the dynamics of the separation process. This has in turn been utilized to formulate a general operation point strategy when conflicting process objectives are considered.

The negative impact of process disturbances has been investigated for batch chromatographic separation of middle REEs, and it has been shown that the process is very sensitive towards disturbances. A robust optimization method has been presented and implemented to secure that the number of failed batches were kept at an acceptable level for a certain degree of process disturbances, and expected performance changes due to the process robustification have been provided. The robust optimization study also provided insights concerning the process' low robustness, and it was found that it is largely due to the neighbouring peaks' proximity to the product pooling horizon.

6.2 Future work

Future experimental work should include studies that verify the model based optimal operation points, and it would also be interesting to carry out REE separation experiments with a two-column MCSGP setup. When it comes to multi-objective optimizations, it would be interesting to investigate if the performance can be pushed even further by applying nonlinear elution gradients. In addition to this, it would be interesting to apply optimizations on further REE mixtures and investigate how the process changes when the source of raw material changes, *i.e.* when the REE ore composition changes.

The process robustification can potentially be improved in terms of performance by applying the presented robust optimization method in conjunction with the variable pooling cut time control strategy as described in [65]. It should be pointed out that the presented robust optimization method targets process parameter settings and considers parameter variations at the process design stage, whereas the variable pooling control strategy allows for changing cut times during operation to compensate for process parameter variations. The idea here would be to utilize the increased pooling cut time flexibility from the variable pooling control strategy to allow the presented robust optimization method to push the operating points further towards ideal optimal performance already at the design stage.

Finally, it would be of interest to apply the presented robust optimization method on an MCSGP process as well as on other chromatography applications than REE.

Bibliography

[1] Andersson, N. (2014). *Parallel computing in model-based process engineering*. PhD thesis, Lund University.

[2] Andersson, N., Knutson, H.-K., Max-Hansen, M., Borg, N., and Nilsson, B. (2014). Model-based comparison of batch and continuous preparative chromatography in the separation of rare earth elements. *Industrial & Engineering Chemistry Research*, 53(42):16485–16493.

[3] Aumann, L. and Morbidelli, M. (2007). A continuous multicolumn countercurrent solvent gradient purification (mcsgp) process. *Biotechnology and bioengineering*, 98(5):1043–1055.

[4] Ben-Tal, A., El Ghaoui, L., and Nemirovski, A. (2009). *Robust optimization*. Princeton University Press.

[5] Bhaskar, V., Gupta, S. K., and Ray, A. K. (2000). Applications of multiobjective optimization in chemical engineering. *Reviews in chemical engineering*, 16(1):1–54.

[6] Biegler, L. T. (2010). *Nonlinear programming: concepts, algorithms, and applications to chemical processes*, volume 10. SIAM.

[7] Biegler, L. T., Cervantes, A. M., and Wächter, A. (2002). Advances in simultaneous strategies for dynamic process optimization. *Chemical Engineering Science*, 57(4):575–593.

[8] Bigelius, J. (2013). Study of stationary phases for chromatographic separation of lanthanides. Master's thesis, Lund University.

[9] Borg, N. (2013). *Modeling and Calibration of Preparative Chromatography*. PhD thesis, Lund University.

[10] Borg, N., Westerberg, K., Andersson, N., von Lieres, E., and Nilsson, B. (2013). Effects of uncertainties in experimental conditions on the estimation of adsorption model parameters in preparative chromatography. *Computers & Chemical Engineering*, 55:148–157.

[11] Braverman, D. S. (1992). Determination of rare earth elements by liquid chromatographic separation using inductively coupled plasma mass spectrometric detection. *J. Anal. At. Spectrom.*, 7(1):43–46.

[12] Brooks, C. A. and Cramer, S. M. (1992). Steric mass-action ion exchange: displacement profiles and induced salt gradients. *AIChE Journal*, 38(12):1969–1978.

[13] Castor, S. B. and Hedrick, J. B. (2006). Rare earth elements. *Industrial minerals volume, 7th edition: Society for mining, metallurgy, and exploration, Littleton, Colorado*, pages 769–792.

[14] Chin, C. Y. and Wang, N.-H. L. (2004). Simulated moving bed equipment designs. *Separation & Purification Reviews*, 33(2):77–155.

[15] Close, E. J., Salm, J. R., Bracewell, D. G., and Sorensen, E. (2014). A model based approach for identifying robust operating conditions for industrial chromatography with process variability. *Chemical Engineering Science*, 116:284–295.

[16] Cornel, J., Tarafder, A., Katsuo, S., and Mazzotti, M. (2010). The direct inverse method: A novel approach to estimate adsorption isotherm parameters. *Journal of Chromatography A*, 1217(12):1934–1941.

[17] Das, I. and Dennis, J. E. (1997). A closer look at drawbacks of minimizing weighted sums of objectives for pareto set generation in multicriteria optimization problems. *Structural optimization*, 14(1):63–69.

[18] Degerman, M. (2009). *Design of robust preparative chromatography*. Lund University.

[19] Degerman, M., Westerberg, K., and Nilsson, B. (2009). A model-based approach to determine the design space of preparative chromatography. *Chemical engineering & technology*, 32(8):1195–1202.

[20] Felinger, A., Cavazzini, A., and Guiochon, G. (2003). Numerical determination of the competitive isotherm of enantiomers. *Journal of Chromatography A*, 986(2):207–225.

[21] Golev, A., Scott, M., Erskine, P. D., Ali, S. H., and Ballantyne, G. R. (2014). Rare earths supply chains: Current status, constraints and opportunities. *Resources Policy*, 41:52–59.

[22] Golshan-Shirazi, S. and Guiochon, G. (1992). Comparison of the various kinetic models of non-linear chromatography. *Journal of Chromatography A*, 603(1-2):1–11.

[23] Gu, T., Truei, Y.-H., Tsai, G.-J., and Tsao, G. T. (1992). Modeling of gradient elution in multicomponent nonlinear chromatography. *Chemical engineering science*, 47(1):253–262.

[24] Guiochon, G., Felinger, A., and Shirazi, D. G. (2006). *Fundamentals of preparative and nonlinear chromatography*. Academic Press.

[25] Gupta, C. K. and Krishnamurthy, N. (2004). *Extractive metallurgy of rare earths*. CRC press.

[26] Han, K. N., Kellar, J. J., Cross, W. M., and Safarzadeh, S. (2014). Opportunities and challenges for treating rare-earth elements. *Geosystem Engineering*, 17(3):178–194.

[27] Henderson, P. (2013). *Rare earth element geochemistry*. Elsevier.

[28] Hernández González, C., Cabezas, A. J. Q., and Díaz, M. F. (2005). Preconcentration and determination of rare-earth elements in iron-rich water samples by extraction chromatography and plasma source mass spectrometry (icp-ms). *Talanta*, 68(1):47–53.

[29] Holmqvist, A., Andersson, C., Magnusson, F., and Åkesson, J. (2015a). Methods and tools for robust optimal control of batch chromatographic separation processes. *Processes*, 3(3):568–606.

[30] Holmqvist, A., Magnusson, F., and Nilsson, B. (2015b). Dynamic multi-objective optimization of batch chromatographic separation processes. In *12th International Symposium on Process Systems Engineering and 25th European Symposium on Computer Aided Process Engineering*, volume 37, pages 815–820. Elsevier.

[31] Ireland, T., Tissot, F., Yokochi, R., and Dauphas, N. (2013). Teflon-hplc: A novel chromatographic system for application to isotope geochemistry and other industries. *Chem. Geol.*, 357:203–214.

[32] Jakobsson, N., Degerman, M., and Nilsson, B. (2005). Optimisation and robustness analysis of a hydrophobic interaction chromatography step. *Journal of Chromatography A*, 1099(1):157–166.

[33] James, F., Sepúlveda, M., Charton, F., Quiñones, I., and Guiochon, G. (1999). Determination of binary competitive equilibrium isotherms from the individual chromatographic band profiles. *Chemical Engineering Science*, 54(11):1677–1696.

[34] Karlsson, D., Jakobsson, N., Axelsson, A., and Nilsson, B. (2004). Model-based optimization of a preparative ion-exchange step for antibody purification. *Journal of Chromatography A*, 1055(1):29–39.

[35] Kifle, D., Wibetoe, G., Frøseth, M., and Bigelius, J. (2013). Impregnation and characterization of high performance extraction columns for separation of metal ions. *Solvent Extraction and Ion Exchange*, 31(6):668–682.

[36] Knutson, H.-K., Holmqvist, A., and Nilsson, B. (2015). Multi-objective optimization of chromatographic rare earth element separation. *Journal of Chromatography A*, 1416:57–63.

[37] Knutson, H.-K., Max-Hansen, M., Jönsson, C., Borg, N., and Nilsson, B. (2014). Experimental productivity rate optimization of rare earth element separation through preparative solid phase extraction chromatography. *Journal of Chromatography A*, 1348:47–51.

[38] Krättli, M., Müller-Späth, T., Ulmer, N., Ströhlein, G., and Morbidelli, M. (2013). Separation of lanthanides by continuous chromatography. *Industrial & Engineering Chemistry Research*.

[39] Kronholm, B., Anderson, C. G., and Taylor, P. R. (2013). A primer on hydrometallurgical rare earth separations. *Jom*, 65(10):1321–1326.

[40] Ling, L. and Wang, N.-H. L. (2015). Ligand-assisted elution chromatography for separation of lanthanides. *Journal of Chromatography A*, 1389:28–38.

[41] Logist, F., Houska, B., Diehl, M., and Van Impe, J. F. (2011). Robust multi-objective optimal control of uncertain (bio) chemical processes. *Chemical Engineering Science*, 66(20):4670–4682.

[42] Logist, F., Van Erdeghem, P., and Van Impe, J. (2009). Efficient deterministic multiple objective optimal control of (bio) chemical processes. *Chemical Engineering Science*, 64(11):2527–2538.

[43] Massari, S. and Ruberti, M. (2013). Rare earth elements as critical raw materials: Focus on international markets and future strategies. *Resources Policy*, 38(1):36–43.

[44] Max-Hansen, M., Knutson, H.-K., Jönsson, C., Degerman, M., and Nilsson, B. (2015). Modeling preparative chromatographic separation of heavy rare earth elements and optimization of thulium purification. *Advances in Materials Physics and Chemistry*, 5(05):151.

[45] Max-Hansen, M., Ojala, F., Kifle, D., Borg, N., and Nilsson, B. (2011). Optimization of preparative chromatographic separation of multiple rare earth elements. *J. Chromatogr. A*, 1218(51):9155–9161.

[46] McGill, I. (2000). Rare earth elements. *Ullmann's encyclopedia of industrial chemistry*.

[47] Mota, J. P., Araújo, J. M., Rodrigues, R., et al. (2007). Optimal design of simulated moving-bed processes under flow rate uncertainty. *AIChE journal*, 53(10):2630–2642.

[48] Nagrath, D., Bequette, B. W., Cramer, S., and Messac, A. (2005). Multiobjective optimization strategies for linear gradient chromatography. *AIChE journal*, 51(2):511–525.

[49] Nassar, N., Du, X., and Graedel, T. (2015). Criticality of the rare earth elements. *Journal of Industrial Ecology*.

[50] Nestola, P., Silva, R. J., Peixoto, C., Alves, P. M., Carrondo, M. J., and Mota, J. P. (2015). Robust design of adenovirus purification by two-column, simulated moving-bed, size-exclusion chromatography. *Journal of biotechnology*, 213:109–119.

[51] Ojala, F., Max-Hansen, M., Kifle, D., Borg, N., and Nilsson, B. (2012). Modelling and optimisation of preparative chromatographic purification of europium. *J. Chromatogr. A*, 1220:21–25.

[52] Ramzan, M., Kifle, D., and Wibetoe, G. (2015). Comparative study of stationary phases impregnated with acidic organophosphorus extractants for hplc separation of rare earth elements. *Separation Science and Technology*, (just-accepted).

[53] Schmidt-Traub, H., Schulte, M., and Seidel-Morgenstern, A. (2012). *Preparative Chromatography*. Wiley-VCH, Weinheim, 2 edition.

[54] Seidel-Morgenstern, A. (2004). Experimental determination of single solute and competitive adsorption isotherms. *Journal of Chromatography A*, 1037(1–2):255–272.

[55] Siekierski, S. and Sochacka, R. (1964). Reversed-phase partition chromatography with di-(2-ethylhexyl) orthophosphoric acid as the stationary phase : Part ii. factors affecting the height of the plate. *J. Chromatogr. A*, 16(0):385 – 395.

[56] Silva, R. J., Rodrigues, R. C., and Mota, J. P. (2012). Relay simulated moving bed chromatography: Concept and design criteria. *Journal of Chromatography A*, 1260:132–142.

[57] Sivaraman, N., Kumar, R., Subramaniam, S., and Vasudeva Rao, P. (2002). Separation of lanthanides using ion-interaction chromatography with hdehp coated columns. *J. Radioanal. Nucl. Chem.*, 252(3):491–495.

[58] Snyman, J. A. (2005). *Practical mathematical optimization: an introduction to basic optimization theory and classical and new gradient-based algorithms*, volume 97. Springer.

[59] Sochacka, R. and Siekierski, S. (1964). Reversed-phase partition chromatography with di-(2-ethylhexyl) orthophosphoric acid as the stationary phase: Part i. separation of rare earths. *J. Chromatogr. A*, 16:376–384.

[60] Sreedhar, B., Wagler, A., Kaspereit, M., and Seidel-Morgenstern, A. (2013a). Optimal cut-times finding strategies for collecting a target component from overloaded elution chromatograms. *Computers & Chemical Engineering*, 49:158–169.

[61] Sreedhar, B., Wagler, A., Kaspereit, M., and Seidel-Morgenstern, A. (2013b). Optimal cut-times finding strategies for collecting a target component from overloaded elution chromatograms. *Computers & Chemical Engineering*, 49:158–169.

[62] Stegen, K. S. (2015). Heavy rare earths, permanent magnets, and renewable energies: An imminent crisis. *Energy Policy*, 79:1–8.

[63] Storn, R. and Price, K. (1997). Differential evolution–a simple and efficient heuristic for global optimization over continuous spaces. *Journal of global optimization*, 11(4):341–359.

[64] Thakur, N. (2000). Separation of rare earths by solvent extraction. *Miner. Process. Extr. Metall. Rev.*, 21(1-5):277–306.

[65] Westerberg, K., Borg, N., Andersson, N., and Nilsson, B. (2012). Supporting design and control of a reversed-phase chromatography step by mechanistic modeling. *Chemical Engineering & Technology*, 35(1):169–175.